UNIVERSITY OF MINNESOTA
ST. ANTHONY FALLS HYDRAULIC LABORATORY

Project Report No. 356

Temperature and Dissolved Oxygen Simulations for a Lake with Ice Cover

by

Xing Fang and Heinz G. Stefan

Prepared for

U.S. ENVIRONMENTAL PROTECTION AGENCY
Environmental Research Laboratory
Duluth, MN 55804
St. Paul, Minnesota

December, 1994

Acknowledgements

David Wright, Minnesota Department of Natural Resources, provided measurements of water temperatures, dissolved oxygen concentrations, ice and snow thicknesses for Thrush Lake from 1986 to 1991. Patrick Brezonik and Carolyn Sampson, Department of Civil Engineering, University of Minnesota, provided measurements of water temperatures, dissolved oxygen concentrations, ice and snow thicknesses for Little Rock Lake, Wisconsin, from 1983 to 1993. We are grateful to have received these data.

This study was supported by a grant from the U.S. Environmental Protection Agency/ERLD. John G. Eaton was project officer. J. Howard McCormick of the USEPA/ERLD reviewed the manuscript and made numerous valuable suggestions.

Table of Contents

List of Symbols

A	horizontal area of a control volume or a layer (m^2);
A_s	surface area of a lake (m^2);
A_{SED}	sediment surface area (m^2);
BOD	biochemical oxygen demand (mg L^{-1});
C	dissolved oxygen concentration (mg L^{-1}) or a constant;
Chla	chlorophyll-a concentration (mg L^{-1});
c_p	heat capacity (kcal kg^{-1} $°C^{-1}$);
C_s	saturated dissolved oxygen concentration at the surface temperature (mg L^{-1});
C_{sw}	snow compacting coefficient;
C_w	empirical coefficient for h_{sa} (-);
C_{w1}	coefficient obtained by least square regression (°c);
C_{w2}	coefficient obtained by least square regression (cm);
D.O.	dissolved oxygen;
e_a	vapor pressure of the air (mbar);
e_s	saturated vapor pressure above the snow surface (mbar);
F_s	oxygen flux due to surface reaeration (mg O_2 m^{-2} day^{-1});
g	acceleration due to the gravity (m s^{-2});
h_{sa}	bulk heat transfer coefficient (BUT hr^{-1} ft^{-2} $°F^{-1}$);
H_a	heat flux due to atmospheric long wave radiation (kcal m^{-2} day^{-1});
H_{br}	heat flux due to back radiation (kcal m^{-2} day^{-1});
H_c	heat flux due to convection (kcal m^{-2} day^{-1});
H_e	heat flux due to evaporation (kcal m^{-2} day^{-1});
H_{is}	solar radiation flux absorbed in the ice layer (kcal m^{-2} day^{-1});
H_{iw}	heat flux at the ice-water interface (kcal m^{-2} day^{-1});
H_s	net strength of heat sources and sinks per unit volume of sediments (J m^{-3});
H_{sed}	heat flux within lake sediments (kcal m^{-2} day^{-1});
H_{sn}	net solar (short wave) radiation (kcal m^{-2} day^{-1});
H_{sw}	solar radiation flux absorbed in the snow layer (kcal m^{-2} day^{-1});
H_w	net strength of heat sources and sinks per unit volume of water (J m^{-3});
k	thermal conductivity (W m^{-1} $°C^{-1}$);
k_b	first order decay coefficient for BOD (day^{-1});
k_e	surface oxygen transfer coefficient (m day^{-1});
k_r	respiration rate coefficient (day^{-1});
K_s	heat diffusion coefficient of the sediments (m^2 day^{-1});
K_Z,K_{ZW}	vertical thermal turbulent diffusivity of water (m^2 day^{-1});
K_{Zmax}	maximum hypolimnetic diffusivity (m^2 day^{-1});
K_{ZS}	thermal diffusivity of lake sediments (m^2 day^{-1});

$Min[L]$ light limitation factor for photosynthesis (-);
N Brunt-Vaisala frequency (s^{-1})
P photosynthetic oxygen production (mg O_2 day^{-1});
P_{max} maximum photosynthetic oxygen production rate, mg O_2 (mg Chla)$^{-1}$ hr^{-1};
P_r precipitation (m of water day^{-1});
P_{sw} snow fall from given weather data (m day^{-1});
R plant respiration (mg O_2 day^{-1});
S_b sedimentary oxygen demand coefficient (mg O_2 m^{-2} day^{-1});
SOD sedimentary oxygen demand;
t time step (day);
T water temperature (°C);
T_a air temperature (°C);
T_b water temperature at lake bottom (°C);
T_{mean} volume averaged water temperature (°C);
T_m melting point temperature (°C);
T_o sediment temperature at 10 m below the lake bottom (°C);
WOD water column oxygen demand (g O_2 m^{-3} day^{-1});
WODR winter oxygen demand rate (g O_2 m^{-2} day^{-1});
U_a wind speed (m sec^{-1});
V lake volume (m^3);
V_{WODR} volumetric winter oxygen depletion rate (g O_2 m^{-3} day^{-1});
YCHO2 yield coefficient = ratio of mg chlorophyll-a to mg oxygen;
z vertical coordinate (m);
z_m mean depth (m);
Z_{max} maximum depth of a lake (m);
z_s depth upward from the lake bottom (m);
z_w weather station-elevation above the mean sea level (ft);
$\dot{z}_c$ snow depth reduction rate by melting due to convection (m day^{-1});
$\dot{z}_e$ snow depth reduction rate by melting due to evaporation (m day^{-1});
$\dot{z}_r$ snow depth reduction rate by melting due to rainfall (m day^{-1});
$\dot{z}_s$ snow depth reduction rate by melting due to solar radiation (m day^{-1});
$\dot{z}_{ic}$ ice growth/decay rate due to conduction/convection (m day^{-1});
$\dot{z}_{is}$ ice depth reduction rate by melting due to solar radiation (m day^{-1});
$\dot{z}_r$ ice depth reduction rate by melting due to rainfall (m day^{-1});
ΔZ_s thickness of the first (water surface) layer (m);
$\dot{z}_{ir}$ density (kg m^{-3});
α surface reflectivity (-);
β surface absorption coefficient (-);
μ attenuation coefficient (m^{-1});
λ latent heat of fusion (kcal day^{-1});
θ_b temperature adjustment coefficient for BOD (-);

θ_r temperature adjustment coefficient for plant respiration (-);

Subscripts

s	sediment;
w	water;
sw	snow;
i	ice;
iw	ice/water.

List of Figures

List of Tables

1. INTRODUCTION

To project the effect of potential climate change on water quality and ecology of lakes in a region, deterministic simulation models for water temperature and for dissolved oxygen concentration have been developed by Stefan, Hondzo and Fang (1993). The water temperature model is driven by meteorological parameters which act on a lake through the water surface (Fig. 1). In cold regions where lakes are ice-covered in winter, heat and oxygen transfer processes, which normally occur through an open water surface, are substantially altered by winter ice and snow cover. Therefore separate models for winter conditions must be developed. The objective of this report is to describe the development of process-oriented deterministic, one-dimensional winter water temperature and dissolved oxygen models which predict the water quality in a lake from fall through the ice-cover period and into spring. Starting with conditions typical of the end of the open water season, the winter water temperature model must include simulation of cooling of the surface water to freezing conditions, latent heat removal, onset of ice-cover, radiation and conduction heat transfer through ice and snow and water mixing below the ice cover. One of the applications of these models will be to study the effect of low water temperatures and oxygen levels on fish survival and growth in ice-covered lakes under different climate conditions.

Lake water quality models traditionally are for individual lakes and the open water season (DiToro and Connolly, 1980; Riley and Stefan, 1987; Blumberg and DiToro, 1990; Stefan et al., 1992). The models described herein are intended for year-round simulations of regional lake assemblages to determine long term water temperature and dissolved oxygen behavior rather than short time behavior. The difference is that models of individual lakes can usually be calibrated with measurements for at least one or two years, while no data or not enough data may be available when many lakes have to be simulated.

One-dimensional, numerical simulation models for water temperature profiles in cold climate lakes were recently described by Patterson and Hamblin (1988), Gu and Stefan (1990). These models were designed for study of individual lakes and without simulating dissolved oxygen concentration profiles. In this study the winter water temperature model by Gu and Stefan (1990) has been modified in order to simulate winter temperature structures in a set of regional lakes and without recalibration. Modifications include: (a) determination of vertical turbulent diffusion coefficients, (b) inclusion of sediment heat flux for all layers from the water surface

to the lake bottom, and (c) adaptation to the computational scheme proposed by Pivovarov (1972).

A winter dissolved oxygen submodel has also been developed. The model includes photosynthetic oxygen production and water column oxygen demand (biochemical oxygen demand plus sedimentary oxygen demand). Surface gas transfer is set to zero because of the ice cover. Sedimentary oxygen demand is made dependent on lake trophic state based on the study by Mathias and Barica (1980).

Measured water temperature and dissolved oxygen profiles, ice thicknesses, and snow depths for Ryan Lake, Minnesota (1989 and 1990), Thrush Lake, Minnesota (from 1986 to 1991) and Little Rock Lake, Wisconsin (from 1983 to 1991) will be compared to simulations with the modified one-dimensional winter water temperature and dissolved oxygen models. To do this, the winter simulation models have been combined with water temperature (Hondzo and Stefan, 1993) and dissolved oxygen (Fang and Stefan, 1994) models for the open water season to a year-round water temperature and dissolved oxygen model as discussed by Stefan et al. (1994). The simulations start on April 16 of the first year for which data are available, and end on October 31 of the most recent year for which measurements are available. Model parameters/coefficients are kept constant over the entire simulation period. A sensitivity analysis of model results to threshold conditions for ice formation and to weather data will also be presented. Difficulties of water temperature and dissolved oxygen simulations around the freeze-over and ice-out periods will be discussed specifically. Recommendations for future study will be provided.

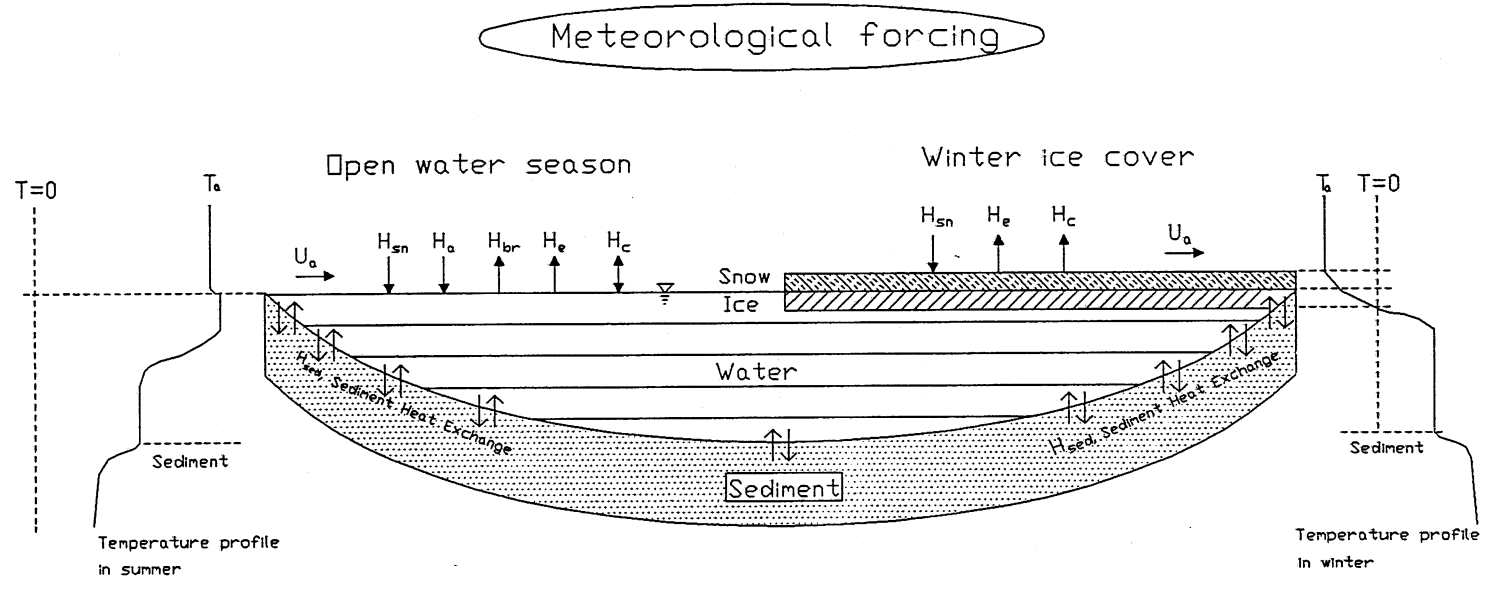

Fig. 1. Schematic of a stratified lake showing heat transfer components and temperature profiles in summer and winter.

2. WINTER WATER TEMPERATURE MODEL DEVELOPMENT

2.1 Previous Work

A one-dimensional, numerical simulation model for water temperature profiles in cold climate lakes was recently described by Gu and Stefan (1990). The model solves the one-dimensional, vertical unsteady heat transfer equation for water in a lake. That equation is

$$\frac{\partial T_w}{\partial t} = \frac{1}{A}\frac{\partial}{\partial z}\left(K_z A \frac{\partial T_w}{\partial z}\right) + \frac{H_w}{\rho c_p} \qquad (1)$$

where T_w (°C) is the water temperature, t (day) is the time, A (m^2) is the horizontal area as a function of depth z (m), K_Z (m^2 day^{-1}) is the vertical turbulent heat diffusion coefficient, ρc_p (J m^{-3} °C^{-1}) represents heat capacity per unit volume and is the density of water (ρ) times heat capacity of water (c_p), and H_w (J m^{-3} day^{-1}) is the heat source or sink strength per unit volume. Radiation absorption inside the water column (H_w) is a heat source term. Heat exchange (flux) between the water and sediments, although a boundary condition, is treated as a contribution to the source/sink term only for the bottom layer(s) (Typically it is a sink term during the open water season and a source term during the ice cover period). Similarly heat exchange between the atmosphere and the water (Fig. 1) can be treated as a source/sink term for the topmost water layer in a lake. For the open water season the computational scheme and the determination of source and sink terms have been discussed, e.g. by Ford and Stefan (1980), Hondzo and Stefan (1993), among others. Equation (1) is solved numerically for timesteps of one day and layer thicknesses of one meter.

The vertical diffusion coefficient, $K_Z(z,t)$ in an ice-covered lake, was determined from (Gu and Stefan, 1990):

$$K_z = \min[K_{Zmax}, K_{Zmax} C N^{-1}] \qquad (2)$$

where K_{Zmax} is the maximum hypolimnetic diffusion coefficient and C is the minimum value of N at which the K_{Zmax} occurs (taken to be 8.66×10^{-3} day^{-1}, from Jassby and Powell, 1975), and N is the buoyancy or Brunt-Vaisala frequency defined as

where ρ is the density of water (kg m^{-3}) as a function of depth z and g is the

$$N = \left(\frac{g}{\rho}\frac{d\rho}{dz}\right)^{1/2} \quad (3)$$

acceleration due to the gravity. Equation (2) was developed for the open water season (Mortimer, 1942; Welander, 1967; and Jassby and Powell, 1975). Equation (2) with $K_{Zmax} = 0.023\ m^2 day^{-1}$ was used by Gu and Stefan (1990) for the winter water temperature simulations of Lake Calhoun. According to equation (2) actual K_Z values are reduced by a function of N.

Snow and ice submodels were originally developed by Gu and Stefan (1990) and are summarized in Appendices A and B, respectively. During the ice cover period, the model (Gu and Stefan, 1990) simulates ice and snow thicknesses and sediment temperature profiles (heat conduction equation) first, then determines the heat source/sink term H_w in equation (1), and finally solves the heat transfer equation (1) to obtain water temperatures profiles below the ice. The model uses the heat transfer equation (1) to a stacked layer system consisting of lake sediments, water, ice-cover and snow-cover (Fig. 1). At the air/snow (or air/ice interface when snow is absent) the net heat flux from the atmosphere into or out of the snow/ice cover is calculated. Contributions are made by solar radiation (H_{sn}), evaporation (H_e) and convection (H_c). Air temperature, wind speed, solar radiation, relative humidity, and precipitation (rainfall and snowfall) are used as input parameters. Snow thickness is determined from snow accumulation due to precipitation, followed by a compaction process, and melting on the snow surface due to conduction, convection, rainfall, and long wave radiation, and melting within the snow layer due to absorption of short wave radiation. In the model ice grows at the ice-water interface, it can decay at the snow-ice interface, ice-water interface, and within the ice layer.

Gu and Stefan (1990) applied the simulation model to Lake Calhoun, MN, and compared the results with sparse field data for the winter period 1971/72. The winter simulation model was further validated by Gu and Stefan (1993) with a detailed data set from Ryan Lake, MN. Winter dissolved oxygen model simulations were not included in Gu and Stefan's study (1990). To further improve the predictive ability of the winter temperature model the following modifications were made.

2.2 Water Temperature Model Modifications

2.2.1 Vertical diffusion coefficients

The vertical diffusion coefficient, $K_Z(z,t)$ in an ice-covered lake, is a function of depth z and time t. In the absent of wind, it is not clear what drives vertical diffusion in an ice-covered lake. However, measurements by Ellis et al. (1991) and Ellis and Stefan (1994) give the following picture: K_z values are very low - nearly the

molecular heat conduction - near the underside of the ice-cover and near the lake bed. They are highest in the unstratified bulk of the water. Density stratification which can be measured by the buoyancy frequency or Brunt-Vaisala frequency N suppresses vertical turbulence and hence reduces K_z values. Water temperature T, density ρ, frequency N and vertical turbulent diffusion coefficient K_Z in an ice-covered lake are all interrelated. Typical vertical profiles are shown in Fig. 2.

The vertical diffusion coefficient, K_Z, determined from actual water temperature measurements in a lake with ice cover (Ellis et al., 1991) is used in this study. K_Z (m^2 day^{-1}) is expressed as a function of N.

$$K_Z = 8.98 \times 10^{-4} \, (N^2)^{-0.43} \tag{4}$$

In the simulation model for the water temperature profile N is determined by using the already known water temperature profiles calculated in the previous timestep or by an iteration process. Immediately below the ice cover water temperatures typically increase rapidly from 0°C to a temperature which is often between 3 and 4°C, and depends on the fall cooling process and heat release from the sediments (Ellis and Stefan, 1994). Hence K_Z calculated by eq. (4) typically increases with depth and usually reaches a nearly constant value typically at more than 3 m depth below the ice-water interface. The maximum turbulent diffusion coefficient occurs under weakly stratified conditions, which are defined as $N^2 \leq 7.5 \times 10^{-5}$ sec^{-2} (Hondzo and Stefan, 1993). Hence $K_{Zmax} = 0.065$ m^2 day^{-1}.

Recently Ellis and Stefan (1994) specified the vertical diffusion coefficient K_Z (m^2 day^{-1}) near the lake bottom as

$$K_Z = 100 \, \frac{|H_{sed}|}{\rho c_p C_{W1}} \, (z_s + C_{W2}) \tag{5}$$

where H_{sed} (kcal m^{-2} day^{-1}) is the heat flux from the sediment to the water, z_s (m) is the distance from the sediment-water interface (positive upward), and C_{W1} and C_{W2} are coefficients determined by least square regression analysis (Ellis and Stefan, 1994) to be 0.623°C and 0.65 m, respectively. Equation (5) worked well up to 3 meters above the lake bottom in the lake investigated by Ellis and Stefan (1994). In the new model K_Z is determined at each depth and timestep by eq. (4) downward from the ice-water interface and by eq. (5) upward from the lake bottom. The maximum turbulent diffusion coefficient is used as an upper bound for the K_Z value obtained from (4) and (5).

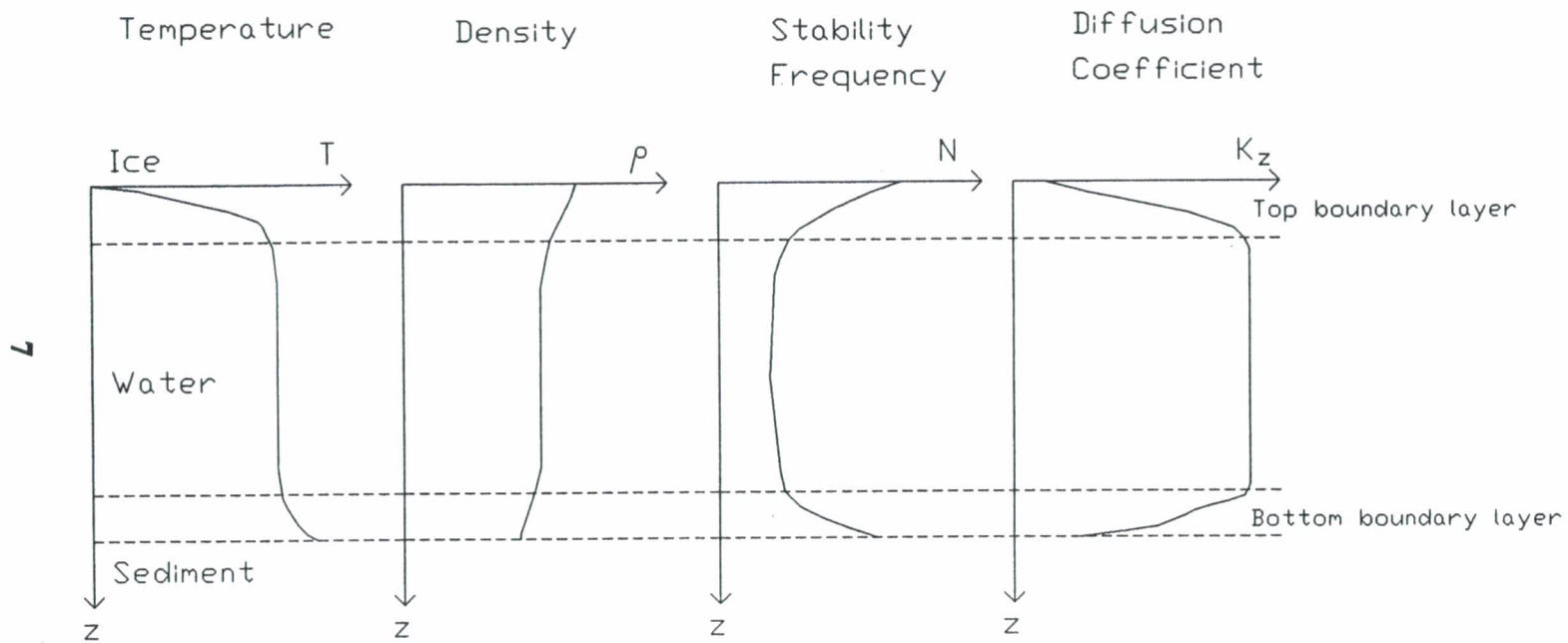

Fig. 2. Schematic of water temperature, density, stability frequency and diffusion coefficient profiles in an ice-covered lake.

2.2.2 Sediment heat transfer

In previous one-dimensional numerical lake water temperature models using discrete layers, heat exchange between the water and sediments was included only for the bottommost water layer(s) (Tsay et al., 1989; Gu and Stefan, 1990). Sediment heat transfer was not considered for all other water layers, although all layers are in contact with sediments (Fig. 1). Sediment heat exchange is of importance, especially during the ice-cover period and in shallow lakes during the open water season. Therefore the sediment heat transfer is included in the new model for all of the layers from the water surface to the lake bottom as schematically shown in Fig. 1 also. In the sediment heat transfer is by conduction and essentially only in vertical direction downward or upward.

To determine the sediment heat flux, the one-dimensional, unsteady heat conduction equation

$$\frac{\partial T_s}{\partial t} = K_S \frac{\partial^2 T_s}{\partial z^2} \tag{6}$$

is solved. T_s (°C) is the sediment temperature and K_s ($m^2\ day^{-1}$) is the heat diffusion coefficient of the sediments. Equation (6) is solved by using an implicit finite difference scheme and applying the following boundary conditions:

$$\begin{aligned} T_s &= T_w(i) && \text{at the lake bottom} \\ \frac{\partial T_s}{\partial z} &= 0 && \text{at 10m below the lake bottom} \end{aligned} \tag{7}$$

$T_w(i)$ is the simulated water temperature in each water layer i at the previous timestep. The first of the two boundary conditions assures continuity of temperatures at the water/sediment interface, the second one implies that seasonal or other temperature fluctuations are damped out at sufficient depth (10m) into the sediments.

The conductive heat exchange flux H_{sed} between the water and sediments was determined from the temperature gradient $(dT_s/dz)_{ws}$ at the sediment/water interface. where k_s is the thermal conductivity of the sediments. The sediment heat fluxes

$$H_{sed} = -k_s \left(\frac{dT_s}{dz} \right)_{ws} \qquad (8)$$

determined by eq. (8) were treated as a source/sink term in the heat balance equation for each water layer in the lake.

2.2.3 Computational scheme

Gu and Stefan's (1990) model simulated first the sediment temperatures below the bottom layer in the lake, using the already known bottom water temperature as a boundary condition, then computed the heat fluxes at the sediment/water interface (lake bottom), and finally simulated water temperatures using the sediment heat flux as a heat source/sink term for the bottom layer. A second boundary condition for the temperature simulations using eq. (1) was the heat flux, $H_{iw} = - k_w (dT_w/dz)_{z=0}$, at the ice-water interface. It was used as a source/sink term for the topmost water layer. In an ice-covered lake turbulent conductive heat transfer coefficient k_w is nearly to the molecular thermal conductivity, but it can change if a density current develops under the ice, e.g. due to spring melt inflow. It is difficult to accurately determine the temperature gradient at the ice-water interface $(dT_w/dz)_{z=0}$. The model by Gu and Stefan (1990) used $\Delta T_w/\Delta z$ instead of $(dT_w/dz)_{z=0}$, and set $\Delta T_w = (T_w)_{\Delta z}$ and $\Delta z = 0.75$ m. The temperature at the ice-water interface was set to 0°C.

In this study the finite difference scheme proposed by Pivovarov (1972) is used to determine the temperature distribution of water and sediments at the same time. The equation for determining the temperature distributions of water and sediments is similar to eq. (1):

$$\frac{\partial T_j}{\partial t} = \frac{1}{A_j} \frac{\partial T_j}{\partial z} \left(A_j K_{z\,j} \frac{\partial T_j}{\partial z} \right) + \frac{H_j}{(\rho c_p)_j} \qquad (j = w, s) \qquad (9)$$

where all quantities relating to water carry subscript w; those relating to the sediments carry subscript s. For the water the horizontal area A_w and the vertical heat diffusion coefficients K_{Zw}, are the same as A(z) and $K_Z(z,t)$ in eq. (1). For the sediment temperature simulations, A_s and K_{Zs} are considered as constant, z is depth below the lake bottom and no internal heat sources or sinks in the sediment exist, i.e. $H_s = 0$. Hence for the sediments equation (9) becomes equation (6). The sediment temperature profiles obtained by solving equation (9) are representative of sediment temperature distribution below the lake bottom layer where $z = z_{max}$ only.

Pivovarov's computational scheme has two fixed boundary conditions: at the ice-water interface and at great depth (taken as 10 m) below the water-sediment interface.

$$T_w = 0 \qquad \text{at } z = 0 \text{ (ice-water interface)} \tag{10}$$

$$T_s = T_0 = \text{constant} \qquad \text{at } z_s = 10 \text{ m} \tag{11}$$

It is not necessary to specify heat flux at the ice-water interface. The boundary condition (11) implies a zero heat flux

$$\frac{\partial T_s}{\partial z} = 0 \qquad \text{at } z_s = 10 \text{ m} \tag{12}$$

In addition a matching condition at the water-sediment interface is necessary:

$$T_w = T_b \quad \text{and} \quad k_w \frac{\partial T_w}{\partial z} = k_s \frac{\partial T_s}{\partial z} \qquad \text{at } z = z_{max} \tag{13}$$

k_w and k_s are the thermal conductivities of the water and sediments, respectively.

The heat exchange (flux) between water and sediment differs from layer to layer because each water layer may have a different temperature (see Fig. 1). It is therefore necessary to solve the sediment heat conduction eq. (6) and to determine the associated sediment/water heat flux from eq. (8) separately for each water layer. This is done using the water temperature calculated for each layer in the previous timestep as a boundary condition. This sediment/water heat flux is then used as a part of the internal source/sink term H_w in eq. (9), which can be solved to give a new water temperature profile in the lake. Another part of H_w in eqs. (1) and (9) is due to internal attenuation of radiation. The vertical radiation distribution within the water column during the ice-cover period is dependent on snow thickness and ice thickness. Therefore water temperatures are simulated by solving eq. (9) together with additional equations for snow and ice as given in detail in Appendices A and B.

3. TEMPERATURE SIMULATIONS (CALIBRATION) FOR THRUSH LAKE

The winter temperature model was combined with a summer temperature model for year round simulations. The summer model has been described by Hondzo and Stefan (1993). This extension to year-round simulations makes it unnecessary to reset initial conditions every year as is done for open water models. The year-round water temperature simulation model was calibrated for Thrush Lake, Minnesota, using data from 1986 to 1991.

3.1 Physiographic Features of Thrush Lake

Thrush Lake is a highly transparent, small lake in Cook County, in northeastern Minnesota (Fig. 3). It is 20 km northwest of Grand Marais, MN. Thrush Lake has a surface area of 66,200 m^2, a maximum mail depth of 14.6 m and a mean depth of 6.85 m (Wright et al., 1989). Thrush Lake was selected for the Acid Precipitation Mitigation Program by the U.S. Fish and Wildlife Service, and monitored by the Minnesota Department of Natural Resources beginning in 1986. From 1986 to 1991, vertical profiles of water temperatures, dissolved oxygen concentrations, underwater light irradiance, chlorophyll-a concentrations as well as Secchi depths and pH were measured at bi-weekly intervals (Wright et al., 1989) during the open water season. The vertical profiles of water temperatures and dissolved oxygen concentrations as well as snow and ice thicknesses were also measured at monthly intervals during four winter periods from 1986 to 1990 (Wright, 1993). Dissolved oxygen concentrations and water temperatures were measured concurrently at 0.5-meter depth intervals using a YSI field meter.

3.2 Simulation Input

Water and sediment temperature profiles and snow/ice thicknesses were simulated by the modified model in daily timesteps. Material properties such as density, specific heat and thermal conductivity were assumed homogeneous and constant for bottom sediments, ice and snow, and were taken from Gu and Stefan (1990) (Table 1). The thermal diffusivity of sediment in the simulation was 0.035 m^2 day^{-1}, slightly larger than that used by Gu and Stefan (1993). The minimum and maximum vertical heat diffusion coefficients of water are the molecular diffusivity (0.012 m^2 day^{-1}) and 0.065 m^2 day^{-1} (N^2 = 0.000075 sec^{-2}), respectively. Two examples of calculated distributions of vertical turbulent diffusion coefficients K_z for Thrush

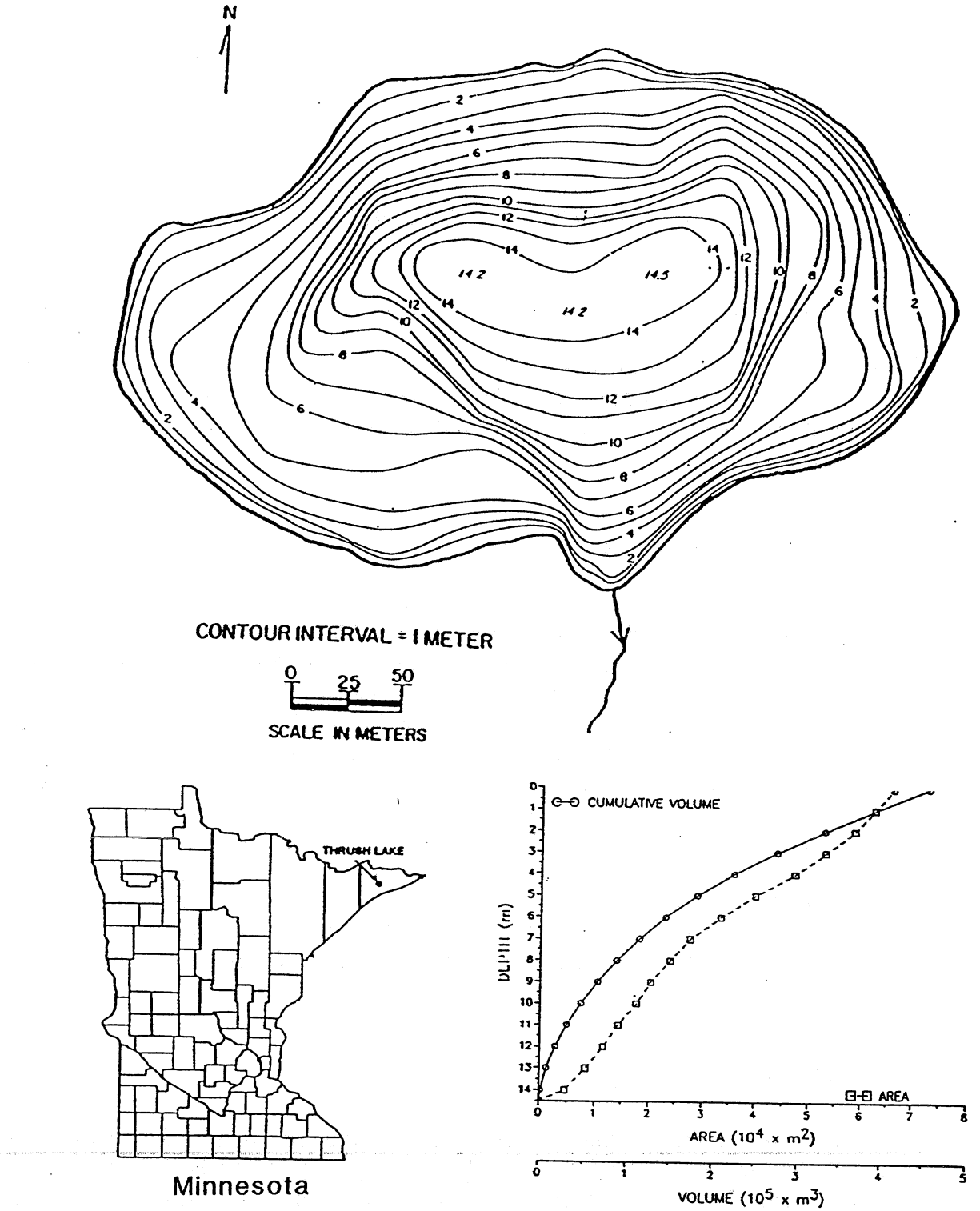

Fig. 3. Bathymetric map, depth-area and depth-volume relationships for Thrush Lake, Cook County, Minnesota. Contour increments are one meter (after Wright, 1989).

Table 1. Material properties used in simulation (after Gu and Stefan, 1990)

Properties	Snow	Ice	Water	Sediment
Density ($kg\ m^{-3}$)	300 (350,400)	920	1000	2300
Heat capacity ($kcal\ kg^{-1}\ °C^{-1}$)	0.50 (0.14)	0.5	1.0	0.24
Thermal conductivity ($W\ m^{-1}\ °C^{-1}$)	0.27 (0.4)	2.6	0.55	0.90
Albedo (-)	0.8 (0.4-0.8)	0.55	-	-
Absorption coefficient (-)	0.34 (0.17-0.34)	0.17 (0.17-0.32)	0.4	-
Extinction coefficient (m^{-1})	40 (20-40)	1.6 (1.6, 7)	0.45	-
Latent heat of fusion ($kcal\ kg^{-1}$)	-	80	597	-

Note: numbers inside parentheses give the range of coefficients or values quoted in other references.

Lake are shown in Fig. 4. Surface solar radiation absorption coefficients, surface reflective and attenuation coefficients of snow and ice were 0.34, 0.8, 40 m^{-1} and 0.18, 0.55, 1.6 m^{-1}, respectively. These values were obtained by model calibration. The snow values are at the upper end of the range specified by Gu and Stefan (1990, Table 1); the ice values are at the lower end, except surface reflectivity. All values agree well with values more recently used by Gu and Stefan (1993). The absorption and attenuation coefficients of water were equal to 0.4 and 0.45 m^{-1}, respectively.

The weather parameters used for the simulations were from the Duluth airport (about 145 km southwest of Thrush Lake), the nearest permanent weather station. The simulation was started with a 4°C isothermal water temperature conditions on April 16, 1986, just after ice-out, and run continuously year by year (both the open water season and the winter ice-cover period), until October 31, 1992 without any modification of model parameters or coefficients.

3.3 Simulation Results

Fig. 5 shows 16 simulated and measured water temperature profiles from 1986 to 1987. There are four profiles for each of the open water seasons and the ice-cover periods in 1986 and 1987. Measured and simulated water temperature profiles show very strong temperature gradients within the top 4 meters below the ice-cover. Water temperature profiles during the melting of lake ice (April) were exactly as discussed by Williams (1969): very steep temperature gradients within 1 meter below the ice-water interface, and a maximum temperature at about 2.0 m below the ice-water interface. At that time solar radiation penetrating through the clear ice (snow has melted) and absorbed in the water contributes significantly to the heating below the ice-water interface. Temperature gradients (increases) with depth near the lake bottom during the ice-cover period are due to heat transfer (conduction) from the sediments.

Fig. 6 shows time-series plots of simulated and measured water temperatures at 1, 4, 7, 10 and 13 m below the water surface or the ice-water interface. Surface water temperatures at 1 and 4 m vary strongly in summer in response to net atmospheric heat inputs (which vary with weather conditions, specifically air temperature and solar radiation). Water temperatures near the lake bottom increase slightly due to sediment heat release in winter and downward heat diffusion of atmospheric heat inputs in summer. Water temperatures in the lower part of the lake drop most significantly during fall turnover. The lowest water temperature near the bed occurs just before the ice cover forms. Statistical analysis of the errors between measurements and simulations of water temperature gave regression coefficients of 0.94, 0.74, 0.96 and standard errors of 1.37, 0.48, 1.07 °C for the open water season, ice-cover period and the total simulation period (1986 - 1991), respectively (Table 2). Values for individual depths are given in Table 2 also.

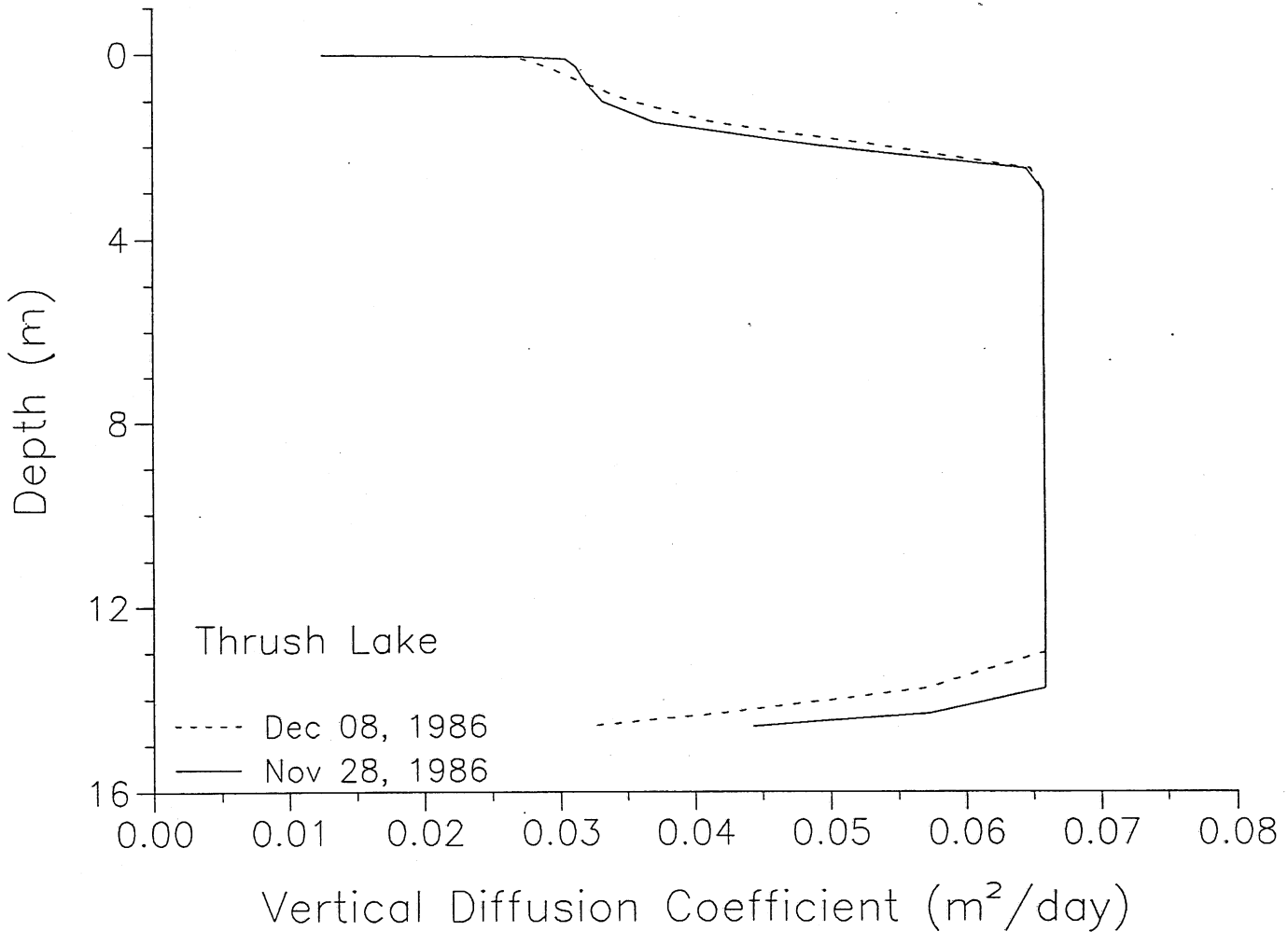

Fig. 4. Examples of the vertical diffusion coefficient (m^2/day) profiles in Thrush Lake during the ice cover period.

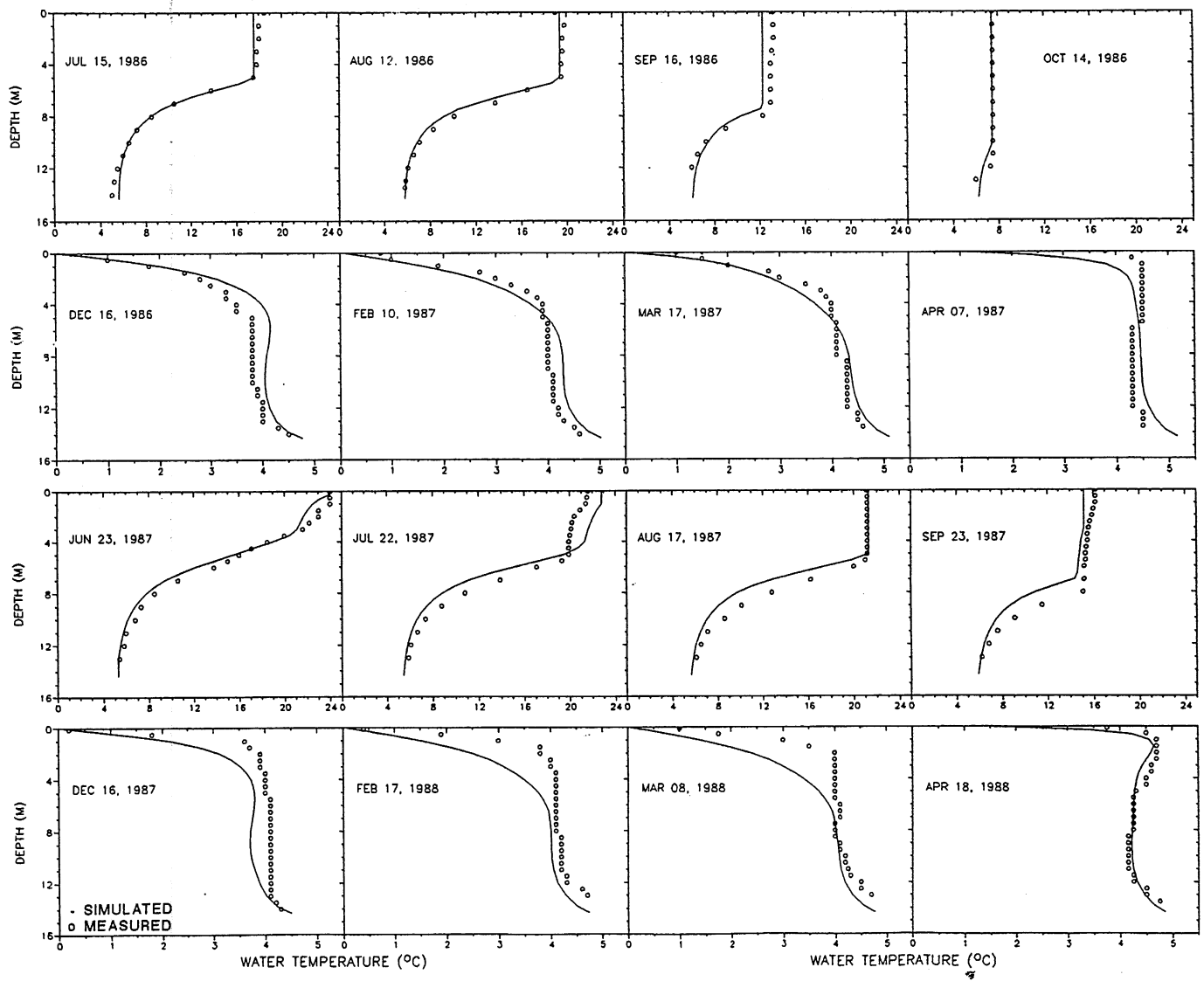

Fig. 5. Simulated (open circles) and measured (solid lines) water temperature profiles in Thrush Lake, Minnesota, from 1986 to 1988.

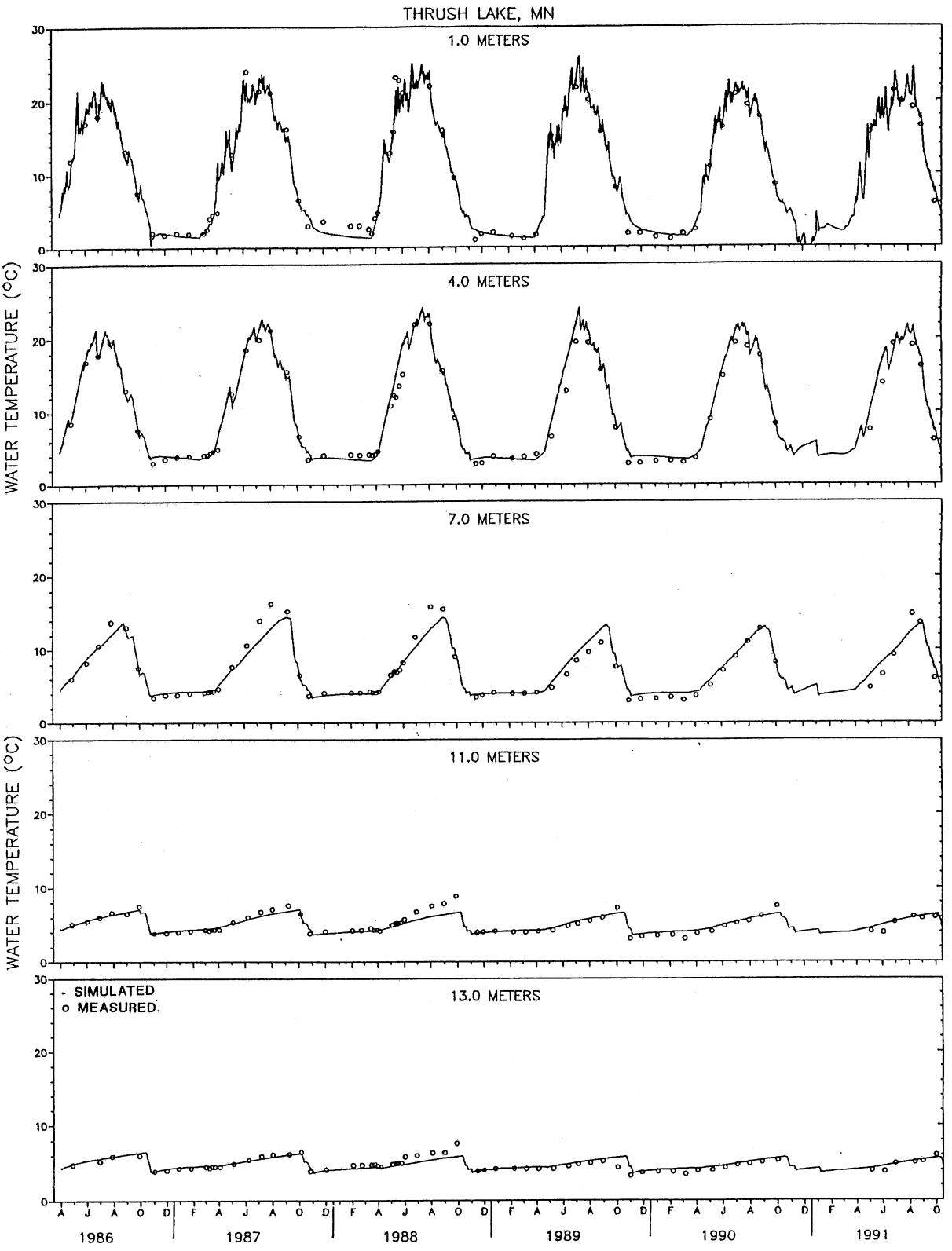

Fig. 6. Time-series plot (1986 - 1991) of simulated and measured water temperatures in Thrush Lake at 1, 4, 7, 11, 13 meters below the water surface or the ice-water interface.

Table 2. Statistics of errors between model simulations and measurements in Thrush Lake, Minnesota.

Water Temperature			Dissolved Oxygen		
Depths	Regression Coefficient	Standard Error (°C)	Depths	Regression Coefficient	Standard Errors (mg L^{-1})
All	0.96	1.07	All	0.51	2.29
Summer	0.94	1.37	Summer	0.47	2.31
Winter	0.74	0.48	Winter	0.54	2.28
z=1 m	0.98	1.27	z=1 m	0.63	1.23
z=4 m	0.95	1.50	z=4 m	0.38	1.48
z=7 m	0.93	1.06	z=7 m	0.36	1.82
z=11 m	0.84	0.58	z=11 m	NA	3.05
z=13 m	0.49	0.49	z=13 m	0.21	2.60

The model produces the best simulation results in summer after a seasonal thermocline has developed, and in winter after a permanent ice cover has formed. The model usually produces the worst simulation results around freeze-over and ice-out time because the physical processes during these periods are more complex than described in the simulation model, and water temperature changes are rapid. To illustrate this point, Fig. 7 shows the strongly divergent simulated and measured water temperature profiles on November 18, 1986 and April 19, 1987, about two or three days after freeze-over and less than a week after ice-out, respectively. Mixing mechanisms during the freeze-over and ice-out periods are particularly difficult to simulate because the density stratification is extremely weak (temperature near 4°C) and wind mixing therefore labile. Fortunately Figs. 5 and 6 show that other simulated water temperature profiles in winter and in the open water season were not significantly affected by the divergences on November 18, 1986, and April 19, 1987. By checking the mixed layer depths in spring, we found that the model simulations for Thrush Lake **missed some of the spring-overturn periods** from 1986 to 1991. This is not very consequential for the water temperature profiles, but affects the dissolved oxygen concentrations near the lake bottom as will be discussed.

Fig. 8 shows the simulated and measured snow and ice thicknesses in two winter periods (1986 to 1988) as well as daily air temperatures and snowfalls at Duluth used for model simulations over those periods. Ice thicknesses in the growth period were simulated well, but there were some underestimations after snowmelt in early spring, possibly because the model does not include a freeze-melt cycle. This usually occurs in early spring when air temperatures vary frequently around 0°C. Snow compacting coefficients typically range from 0.2 to 0.4 (Adams, 1982); a value of 0.35 was obtained by model calibration.

3.4 Sensitivity Analysis

3.4.1 Effect of freeze-over conditions

For winter temperature simulations in lakes, the "threshold conditions" of ice formation are very important. Ashton (Harleman, 1986) introduced the following "threshold conditions" to be met before an intact ice cover is established:

(a) volume averaged water temperature (T_{mean}) is less than 2 °C;
(b) average wind speed over a day is less than 5 m s^{-1};
(c) average daily air temperature is below -5 °C.

Gu and Stefan (1990) found that appropriate conditions to determine the freeze-over date in their winter simulation of Lake Calhoun were (a) 2.65 °C average water temperature, (b) 5 m s^{-1} average wind speed and (c) -2.0 °C average air temperature. Only two vertical profiles during the ice-cover period were available for their model calibration however. Detailed ice/snow thickness measurements did become available

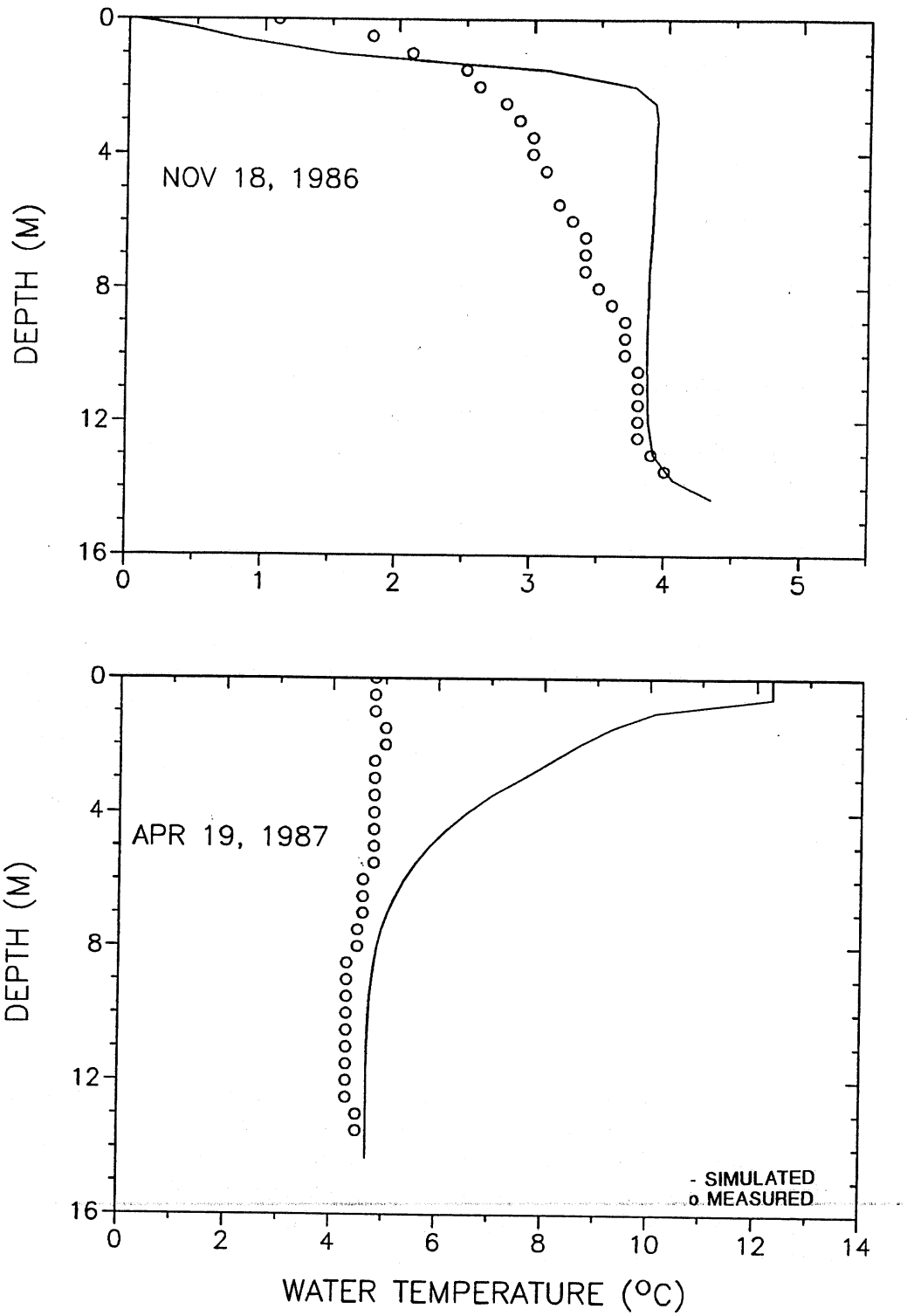

Fig. 7. Simulated and measured water temperature profiles in Thrush Lake on November 18, 1986 and April 19, 1987, respectively.

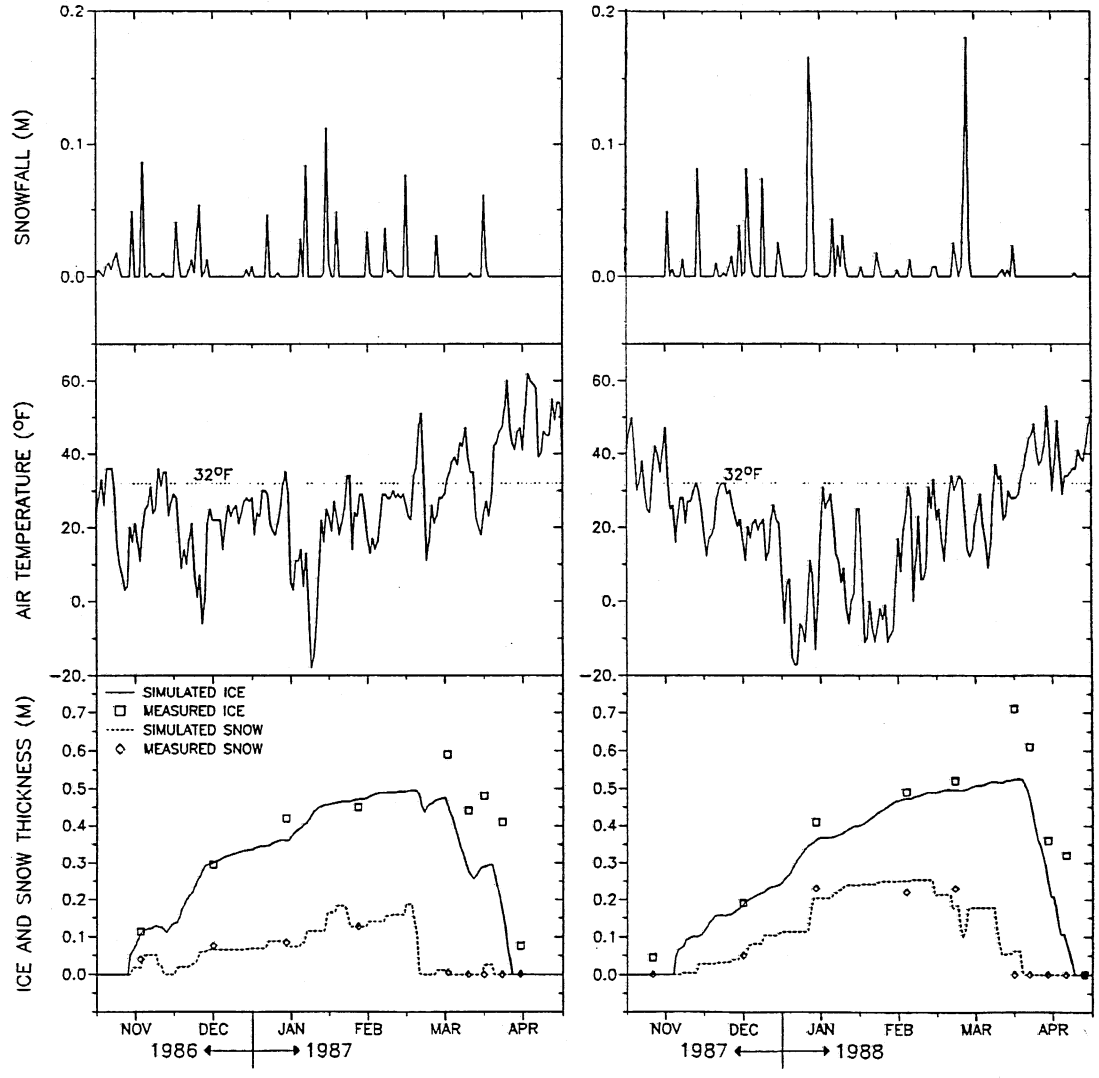

Fig. 8. Simulated and measured ice and snow thicknesses for Thrush Lake (1986 - 1988) and air temperatures and snowfalls at Duluth used in the model simulations.

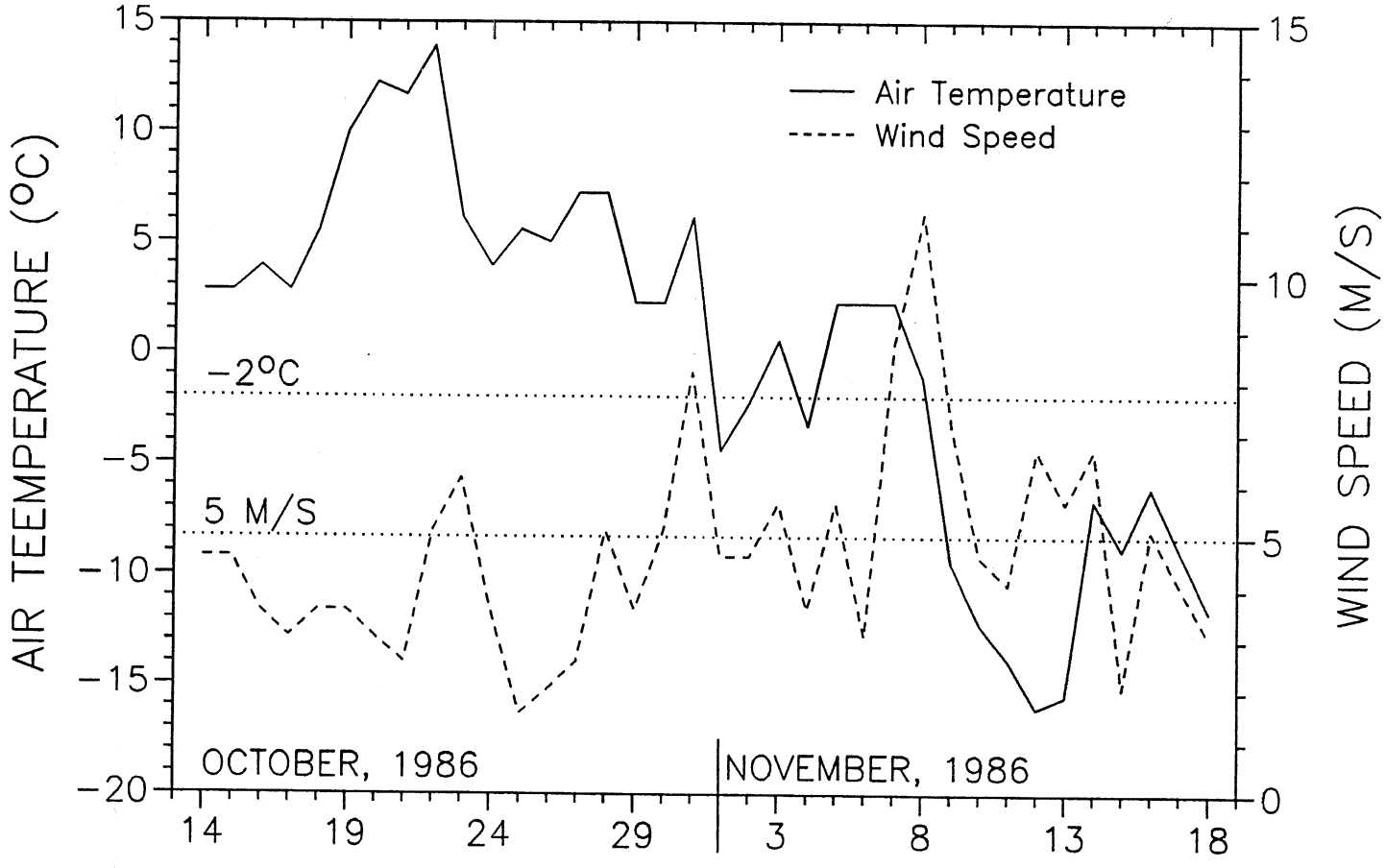

Fig. 9. Air temperatures and wind speeds at Duluth, Minnesota, from October 14 to November 18, 1986.

for Ryan Lake, MN (Ellis et al., 1991; Gu and Stefan, 1993), but no measurements in the open water season were made close to freeze-up. A sensitivity analysis of the freeze-up date to threshold condition could be performed for Thrush Lake, MN, because vertical water temperature profiles during both the open water season and the ice-cover period including ice/snow thicknesses in winter were measured by Wright (1993) from 1986 to 1990.

Fig. 9 shows an example of air temperatures (°C) and wind speeds (m s^{-1}), from October 14, 1986 to November 18, 1986 at Duluth, MN (local weather data were not available for Thrush Lake). These are the dates of the last measurement in the open water and the first measurement under the ice-cover. According to the third threshold condition of ice formation (air temperature below -5 °C), stable ice formation (freeze-up) could occur between November 8, 1986 and November 18, 1986 (minimum air temperature was -16 °C on November 12, 1986). During these ten days the second threshold condition - wind speed less than 5 m s^{-1} - is controlling. According to Fig. 9, the freeze-up could occur on November 10th or 11th, or after November 14th, 1986. A sensitivity analysis of the freeze-up date to the threshold conditions (b) and (c) was not performed. Because these two conditions were well established and documented by Michael (1971) and Ashton (1980, 1986). The threshold conditions (b) and (c) calibrated by Gu and Stefan (1990) were used in this study.

Results of the sensitivity analysis of the freeze-up date to average (volume weighted) water temperature (T_{mean}) are given in Fig. 10. Both simulated and measured ice and snow thicknesses in Thrush Lake, MN are shown. T_{mean} = 3.3 °C was obtained by model calibration, i.e. the best simulations of ice and snow cover in 1986 were achieved. T_{mean} = 3.0 and 3.6 °C were 10% changes from 3.3 °C. Three threshold conditions, T_{mean} = 3.0, 3.3 and 3.6 °C, gave freeze-up dates of December 4th, November 15th and 10th, respectively. With T_{mean} = 3.6 °C, the predicted freeze-up date was several days earlier than the real freeze-up date and the model produced cumulative errors in ice thickness predictions during the growth period. With T_{mean} = 3.0 °C, the predicted freeze-up date is more than 24 days later than the real freeze-up date; the simulated ice thickness grows quickly and catches up with the measurements at a later time. T_{mean} values do not affect snow accumulation predictions when T_{mean} > 3.3 °C, while the simulated snow depths were less than the measurements most of the time at T_{mean} = 3.0 °C. Fig. 11 shows simulated and measured water temperature profiles with three T_{mean} values. Profiles simulated with T_{mean} = 3.3 and 3.6 °C are cooler and warmer than measurements, respectively, and the best results were obtained with T_{mean} = 3.3 °C.

According to Ashton (1986), values of T_{mean} range from 0°C to 4 °C. "For small lakes and ponds the ice cover typically forms some times after the water temperature has cooled to 4°C. The larger and shallower the lake, the more likely that the permanent cover will not form until most of the water body is close to 0°C" (Ashton,

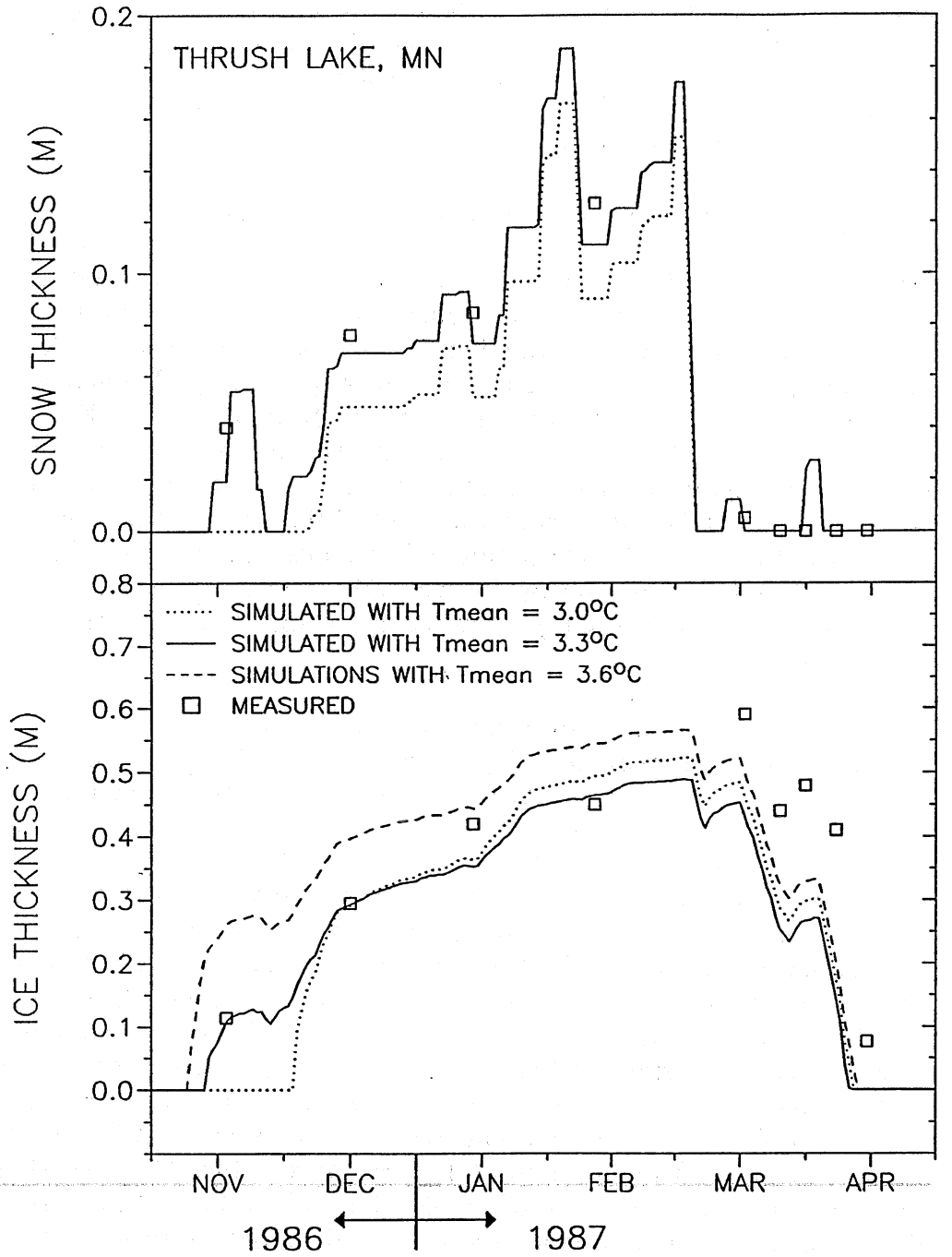

Fig. 10. Simulated snow and ice thicknesses for Thrush Lake (1986 - 1987) using three different threshold conditions (T_{mean}) for ice formation. Measured snow depths and ice thicknesses are given as symbols.

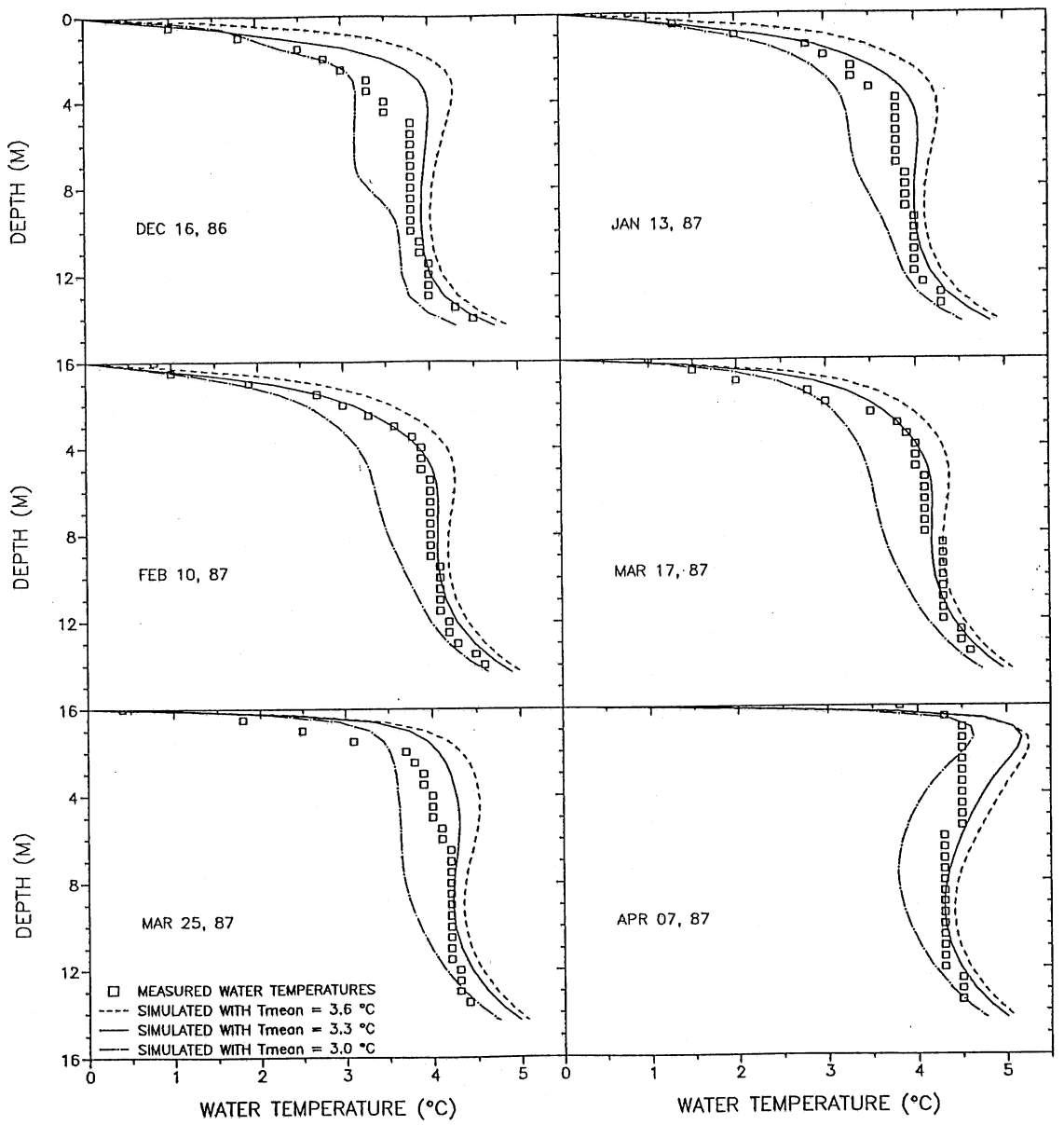

Fig. 11. Simulated water temperature profiles in Thrush Lake using three different threshold conditions (T_{mean}) for ice formation. Measured temperature profiles are given as symbols.

1986). In other words, the critical T_{mean} value is likely related to wind mixing and cooling in fall and hence lake surface area and lake depth. Model calibration for a threshold condition T_{mean} is necessary for a particular lake simulation. This is a weakness, which can be eliminated in further development by considering full heat budget and convective/wind mixing in fall to determine ice formation. Therefore a water temperature model without ice formation threshold conditions needs to be developed for regional lake studies.

3.4.2 Effect of weather conditions

Weather stations are usually not at the lake site, and weather measurements at off-lake stations must be used. The weather data at Duluth (about 145 km southwest of Thrush Lake) and at Ely (about 65 km west of Thrush Lake), MN, were used for a sensitivity analysis. The threshold conditions T_{mean} = 3.3°C for ice formation was used. The results are given in Fig. 12. The ice thicknesses simulated with weather data from Ely, MN, are larger than those with weather data from Duluth, but smaller than measurements. For water temperature simulations in a lake with ice cover, air temperatures are very important and affect ice growth and decay. Two important weather parameters: air temperature and snowfall at Duluth and Ely, MN are given in Fig. 13. Air temperatures at Ely were usually lower (0.5 - 5 °C) than at Duluth, but the basic variability over time is the same. Colder air temperature (Ely) makes Thrush Lake cool more quickly, and hence ice formation starts earlier, ice growth is stronger (Fig. 12). The differences in snowfall in Duluth and Ely are apparent in the snow depths. Fig. 12 tells us that the threshold condition T_{mean} is dependent not only on specific lake geometry but also on weather data used in the simulation.

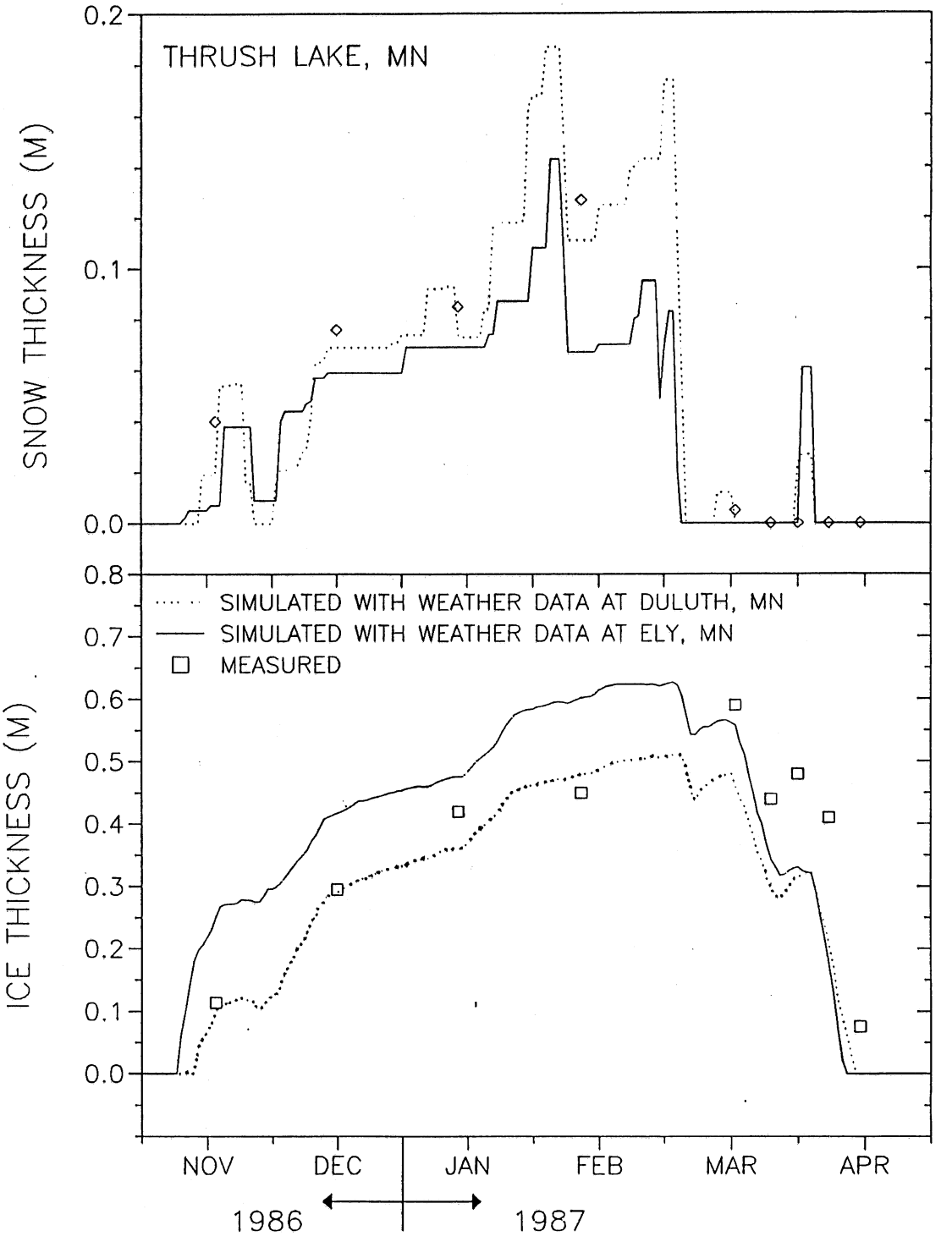

Fig. 12. Simulated snow and ice thicknesses for Thrush Lake (1986 - 1987) using the climate conditions from Ely and Duluth, respectively.

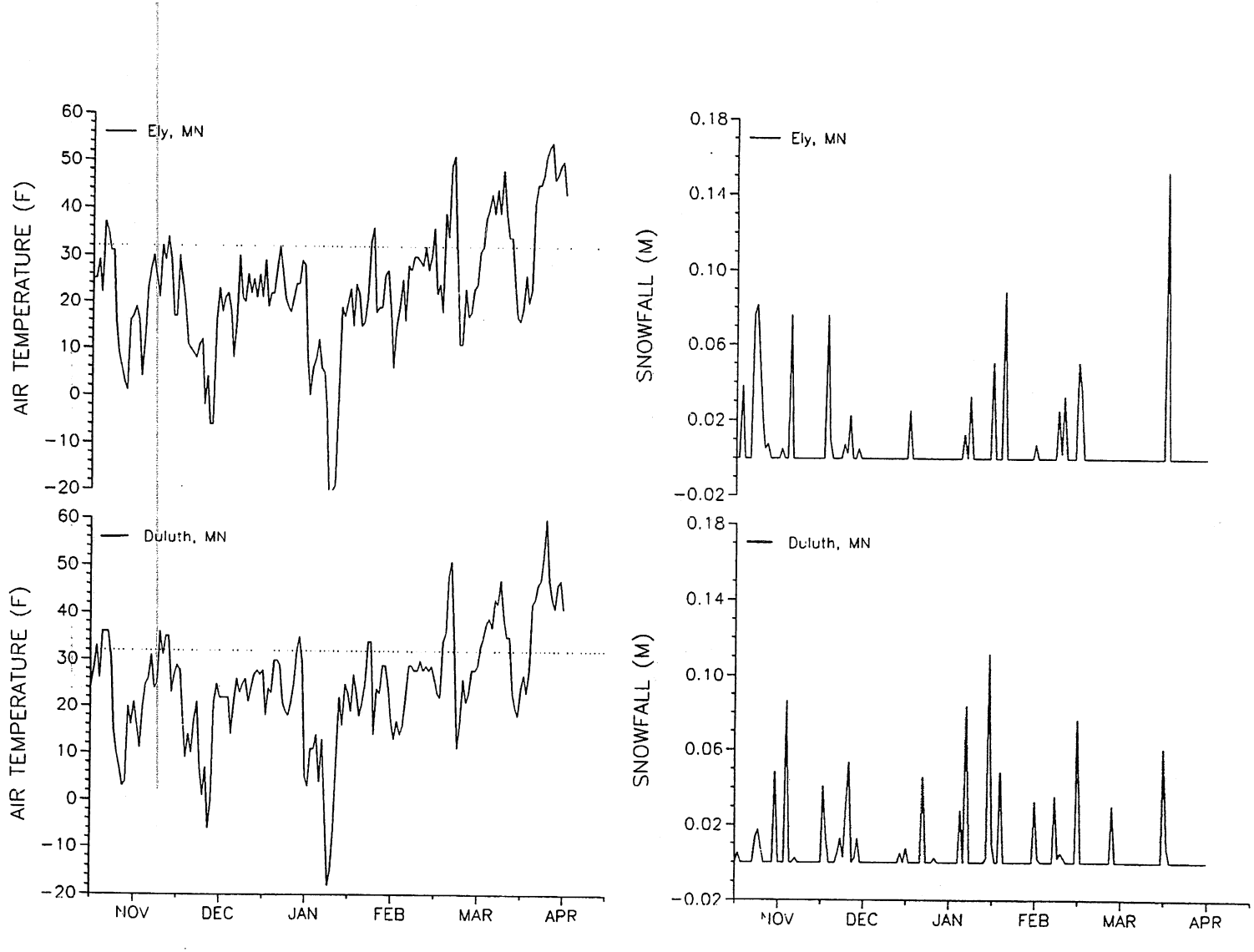

Fig. 13. Air temperatures and snowfalls (1986) at Ely and Duluth, Minnesota, used for the sensitivity analysis.

4. TEMPERATURE SIMULATIONS (VALIDATION) FOR RYAN LAKE AND LITTLE ROCK LAKE

4.1 Validation for Ryan Lake

4.1.1 Physiographic features of Ryan Lake

Ryan Lake, Minnesota, has a surface area of 61,000 m^2, a mean depth of 5.0 meters and a maximum depth of 11.0 meters (Ellis et al., 1990). Thermistors were placed at 0.0, 0.2, 0.4, 0.6, 0.8, 1.0, 1.25, 1.5, 2.0, 2.5, 3.0, 4.0, 5.0, 6.0, 7.0, 8.0, 9.0, 11.0 meters below the air-water or air-ice interface and 0.5, 1.0, 1.5 meters into the sediments to measure temperatures of snow and/or ice, water and sediments. Measurements of the 24 temperatures were made every 2 minutes and averaged and stored every 20 minutes. Theses values were then averaged to obtain daily values for use in model validation. Data were collected from November 15, 1989 to April 3, 1990, a complete ice cover period (Ellis et al., 1991). Ice and snow thicknesses were measured intermittently at about one week intervals. These detailed measurements were used in the validation of the winter water temperature model by Gu and Stefan (1993) and used in this study also.

4.1.2 Validation Results

Figs. 14 and 15 show simulated and measured water temperature profiles in Ryan Lake in the winters of 1989 and 1990. Weather data used for model simulations are from Minneapolis/St. Paul International Airport. From March 23 to April 30, 1989, inflows or density currents existed as discussed by Ellis et al. (1990) and Ellis and Stefan (1994) and were included in the model simulations for Ryan Lake by Gu and Stefan, 1993). The model simulated water temperatures well during two winters. The regression coefficient (R^2) and the standard error between the simulated and measured water temperatures are 0.90 and 1.0 °C, respectively.

Fig. 16 shows simulated ice/snow thicknesses in Ryan Lake from November, 1989 to April, 1990. Regression coefficients and standard errors between simulations and measurements are (0.95, 0.001 m) and (0.96, 0.01 m) for snow and ice thicknesses, respectively. Two important weather parameters, air temperature and snowfall, used in the model simulations, are given at the top of Fig. 16. Ice formed on November 18, 1989, after air temperatures were below 0°C for a week.

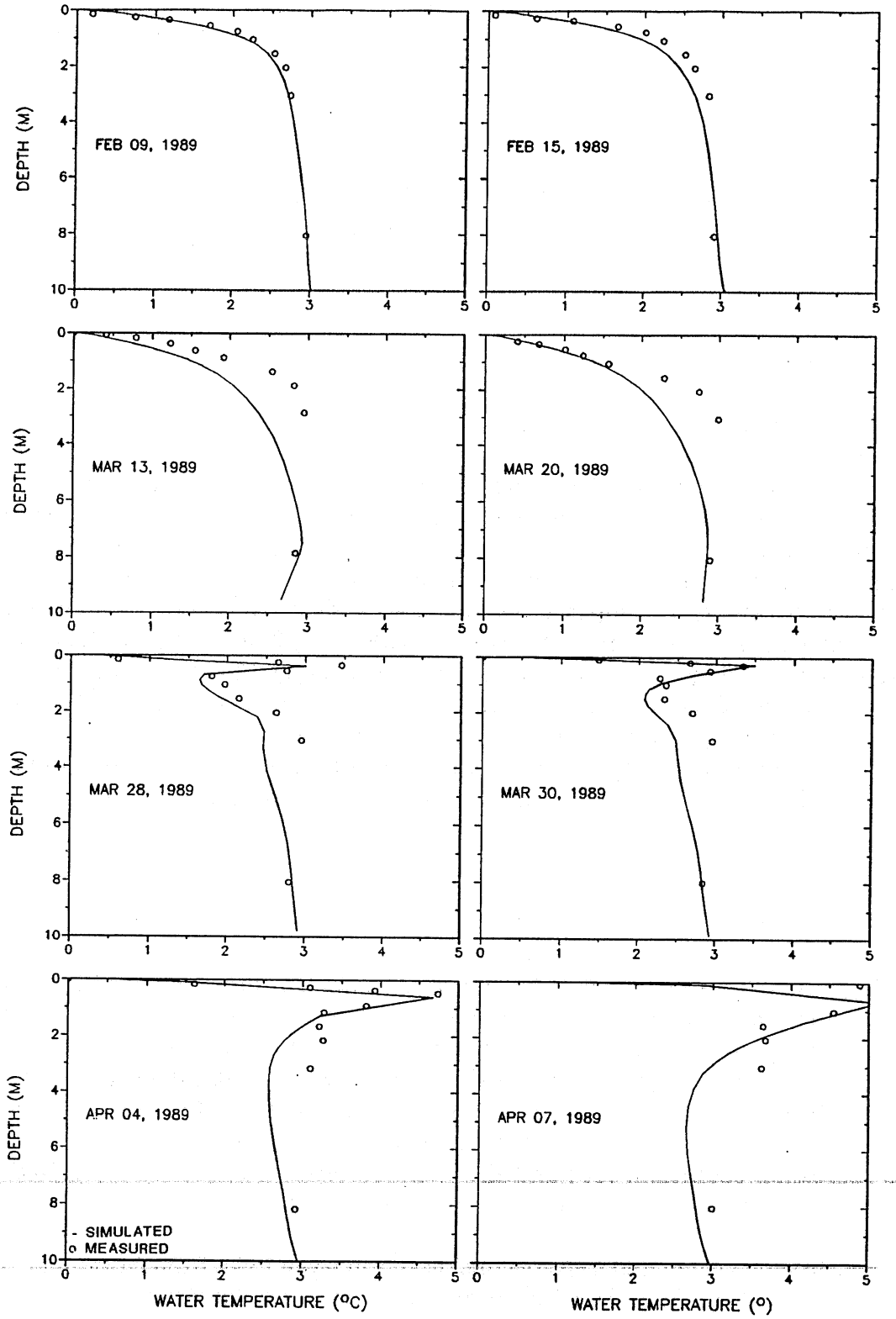

Fig. 14. Simulated and measured water temperature profiles in Ryan Lake, Minnesota, from February to April, 1989 (model validation).

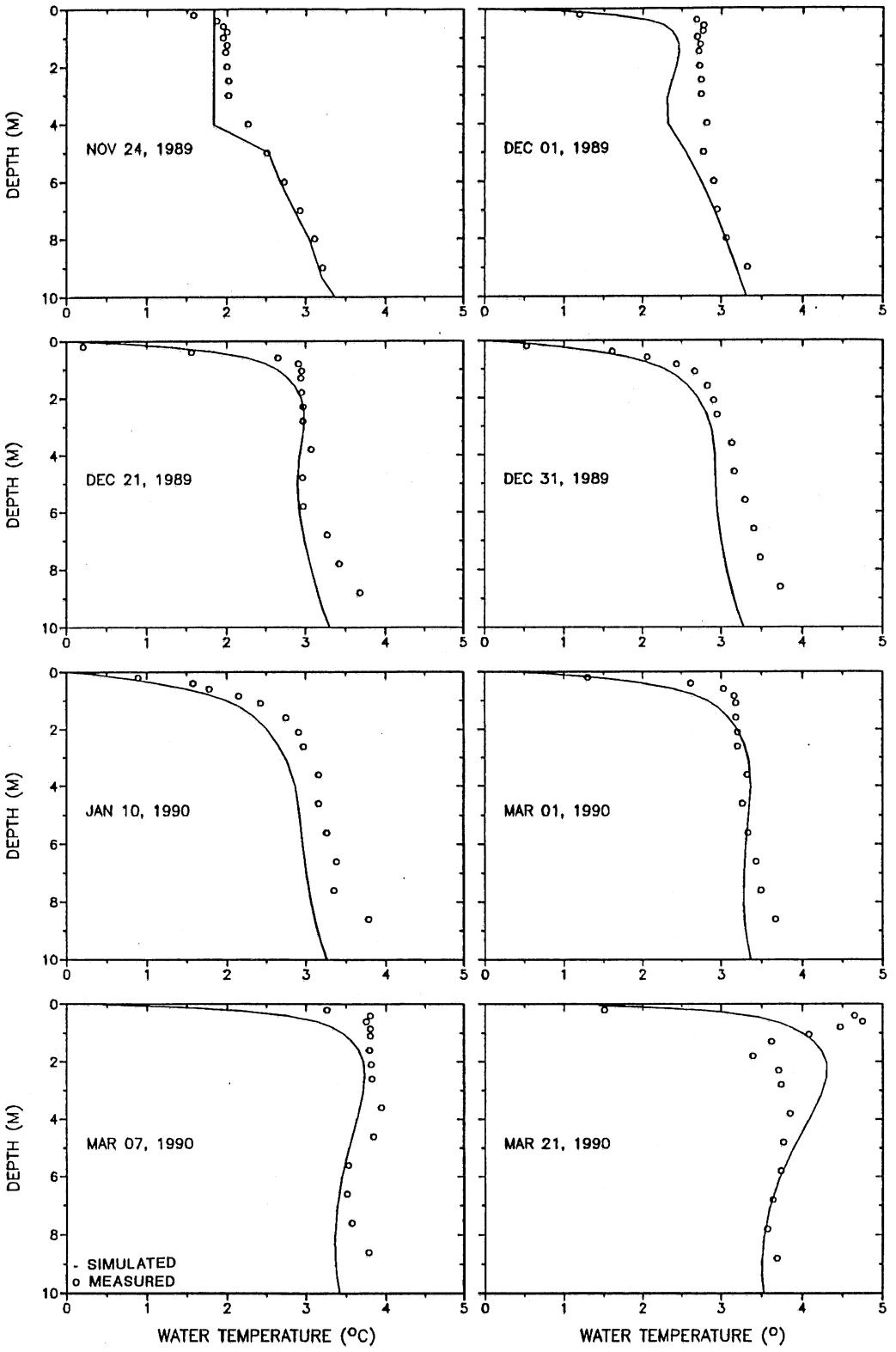

Fig. 15. Simulated and measured water temperature profiles in Ryan Lake, Minnesota, from November, 1989 to April, 1990 (model validation).

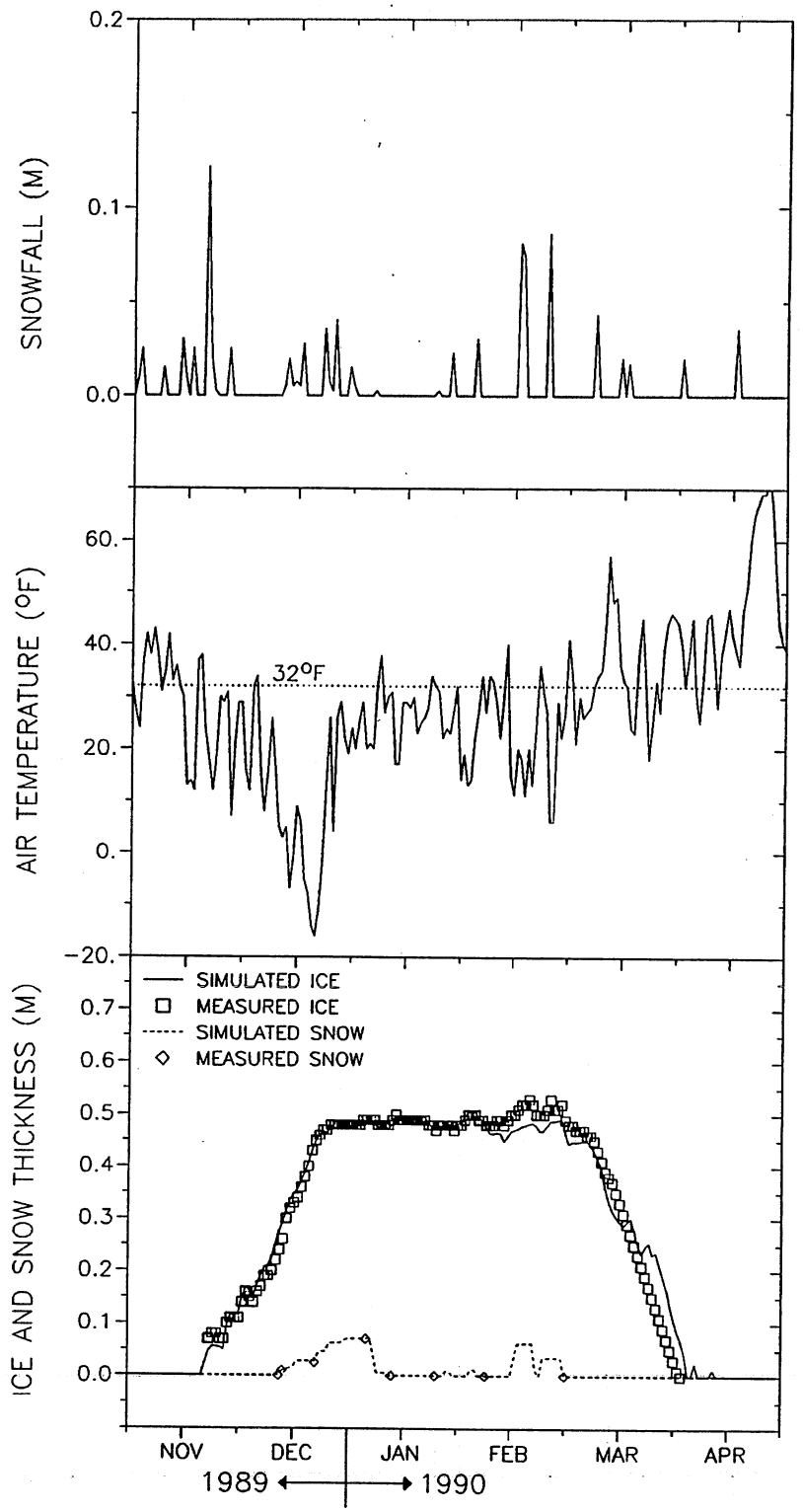

Fig. 16. Simulated and measured ice and snow thicknesses for Ryan Lake, Minnesota, and air temperatures and snowfalls at Minneapolis/St. Paul used in the model validation.

4.2 Validation for Little Rock Lake

4.2.1 Physiographic features of Little Rock Lake

Little Rock Lake is a softwater, oligotrophic seepage lake located in the Northern Highland Lake District in north-central Wisconsin (Sampson, 1992). The lake lies in a small uninhabited, forested watershed. The lake has two main basins that are separated by a narrow constriction (Fig. 17); the two basins are similar in surface area, but the south basin has smaller average and maximum depths than the north basin (Table 3). Little Rock Lake is a groundwater recharge system (no surface inlets or outlets), and it receives most of its water from precipitation directly onto the lake surface (Sampson, 1992). The lake was used for an experimental acidification project from 1983 to 1990 (Brezonik et al., 1985). In August 1984, a Dacron-reinforced polyvinyl barrier was installed at the narrows dividing the two basins as shown in Fig. 17 (Brezonik et al., 1985). Data were collected for nearly two years prior to acidification and for the entire six years of acid additions. Bi-weekly measurements from 1983 to 1991 included water temperatures, dissolved oxygen concentrations, chlorophyll-a concentrations during both the open water season and the ice cover period, ice and snow thicknesses in winter, and many other chemical/biological parameters.

4.2.2 Validation results

Measurements from 1983 to 1991 in Little Rock Lake, WI, were used for the validation of the winter water temperature simulations. North basin and south basin were simulated separately because of their different maximum depths (They were isolated one from the other during the data collection period also). Stratification in the south basin is weak and ephemeral, but the deeper north basin forms a small hypolimnion that represents 6-8% of the total basin volume (Sampson, 1992). The weather data used in the model simulation include air temperatures and precipitation (rainfall and snowfall) from Minocqua, Wisconsin (20 km south of Little Rock Lake), and wind speeds, solar radiation and relative humidity from Duluth airport (200 km northwest of Little Rock Lake), Minnesota. Other parameters and coefficients are the same as used for the simulations of Thrush Lake (Table 1).

Figs. 18A and 18B show time-series plots of simulated and measured water temperatures in both the south and north basins of Littler Rock Lake, respectively. Temperature stratification in the deep north basin of Little Rock Lake is much stronger than in the shallow south basin. Therefore seasonal distributions of both simulated and measured water temperatures in the south basin are quite similar at all depths. In the north basin a distinct hypolimnion exists and its thickness is small.

Table 3. Morphometric characteristics of Little Rock Lake (after Sampson, 1992).

North Basin		South Basin	
Surface Area (m^2)	98000	Surface Area (m^2)	81000
Maximum Depth (m)	10.3	Maximum Depth (m)	6.5
Total Volume (m^3)	380000	Total Volume (m^3)	250000
Contour Depth (meter)	Horizontal Area (m^2)	Contour Depth (meter)	Horizontal Area (m^2)
0	98000	0	81000
1	81000	1	71000
2	64000	2	58000
3	55000	3	40000
4	43000	4	24000
5	32000	5	12000
6	22000	6	4000
7	15400	6.5	0
8	10000		
9	6000		
10	2000		

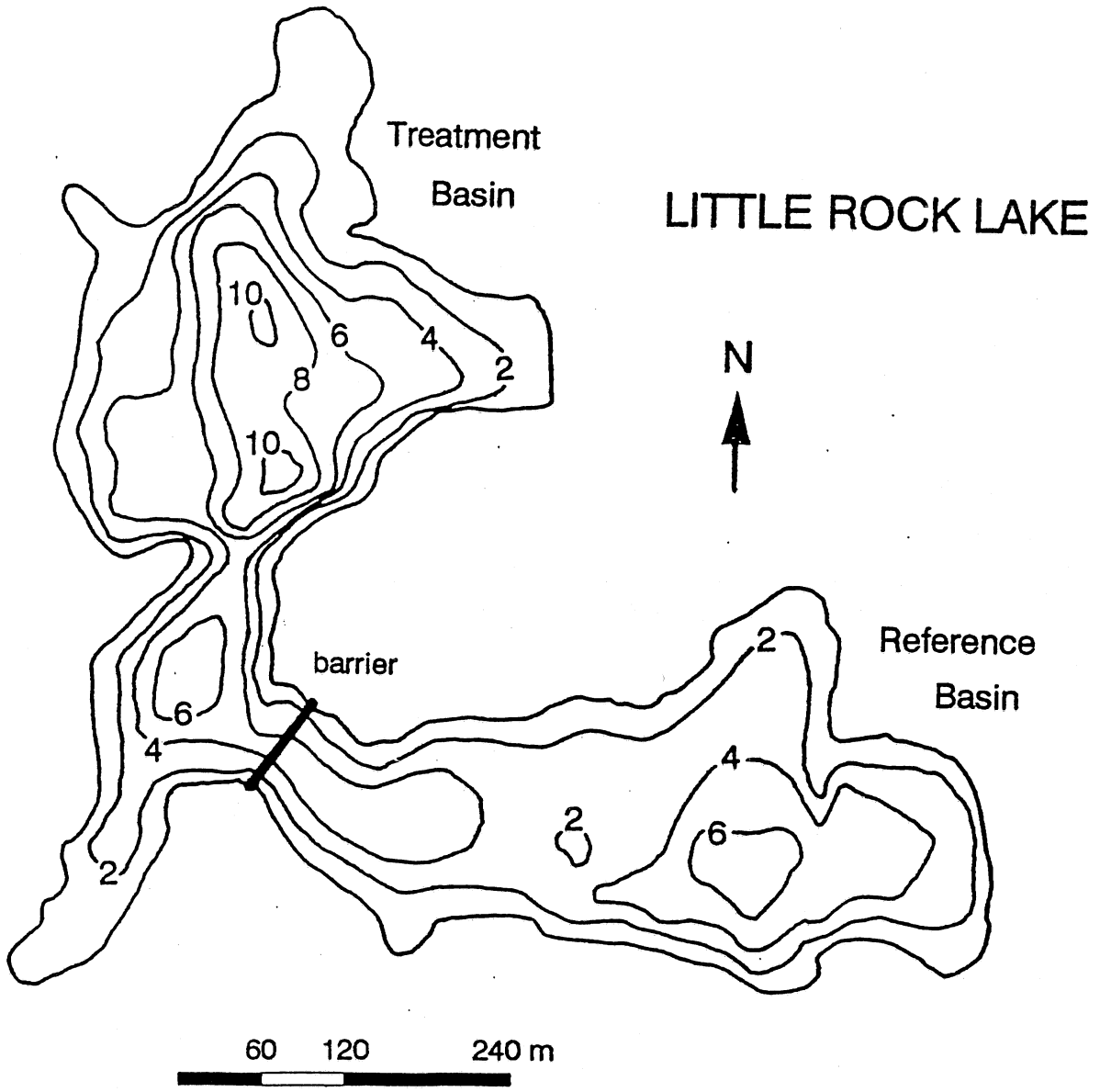

Fig. 17. Bathymetric map of Little Rock Lake, Wisconsin. Contour increments are in 2 meters (from Sampson, 1992).

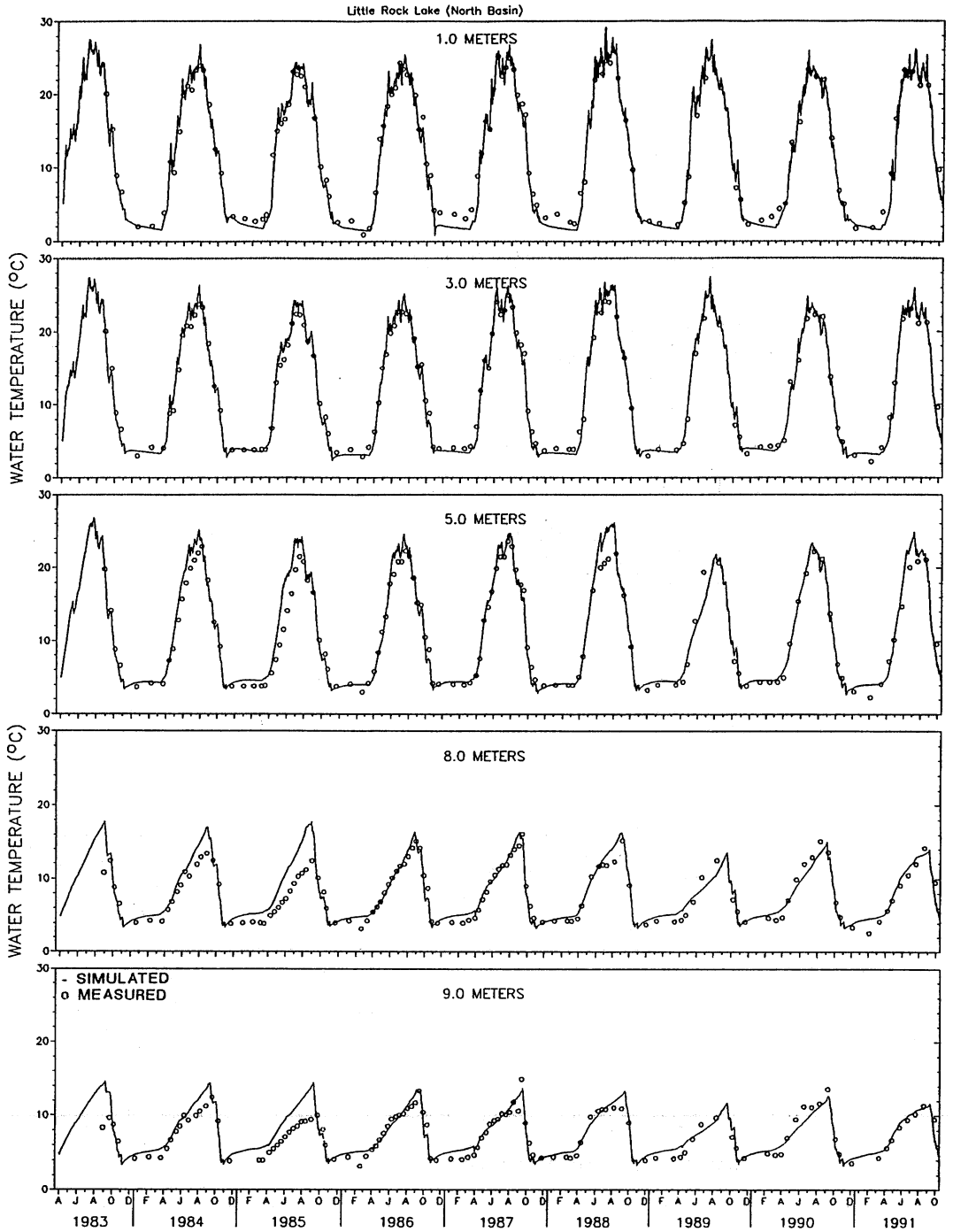

Fig. 18a. Time-series plot (1983-1991) of simulated and measured water temperatures in the north basin of Little Rock Lake at 1, 3, 5, 8 and 9 meters below the water surface or the ice-water interface.

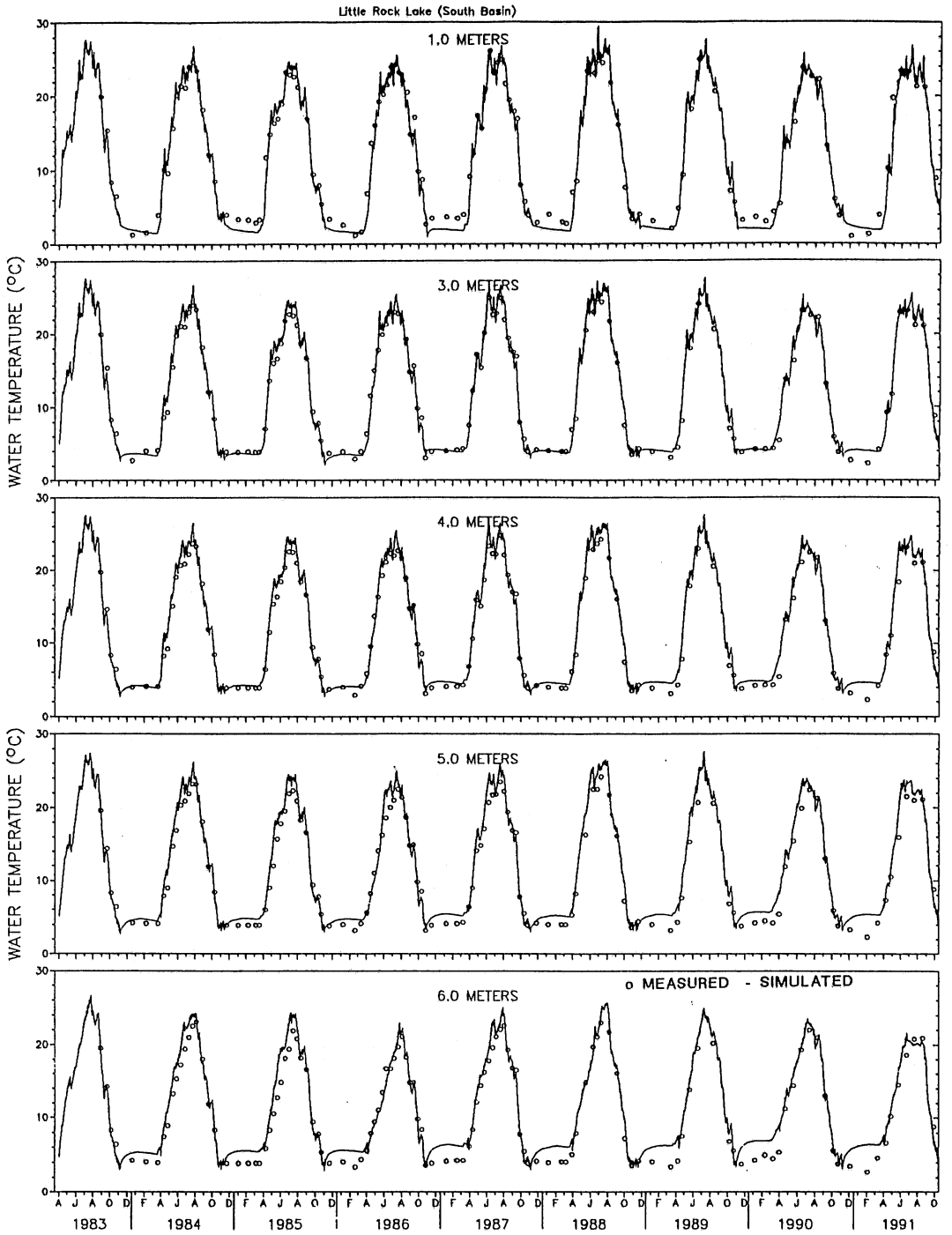

Fig. 18b. Time-series plot (1983-1991) of simulated and measured water temperatures in the south basin of Little Rock Lake at 1, 2, 3, 4 and 5 meters below the water surface or the ice-water interface.

Regression coefficient and standard error between simulated and measured temperatures for all depths are 0.95, 1.51 °C for the south basin and 0.97, 1.41 °C for the north basin, respectively (Fig. 19 and Table 4). During the winter period standard errors between simulated and measured temperatures are 1.0 and 1.29 °C for the north and the south basins, respectively (Table 4). These errors are large relative to the range of water temperatures from 0 °C to slightly larger than 4 °C at the lake bottom. They are due to overpredicted bottom temperatures, especially for the shallow south basin (Fig. 18b). One reason for these overpredictions is that the sediment heat diffusion coefficient (K_s) used in the simulations is probably too small. Heat accumulated in the sediments during the summer can not be quickly released in the fall cooling period and is instead transferred to the water all winter long.

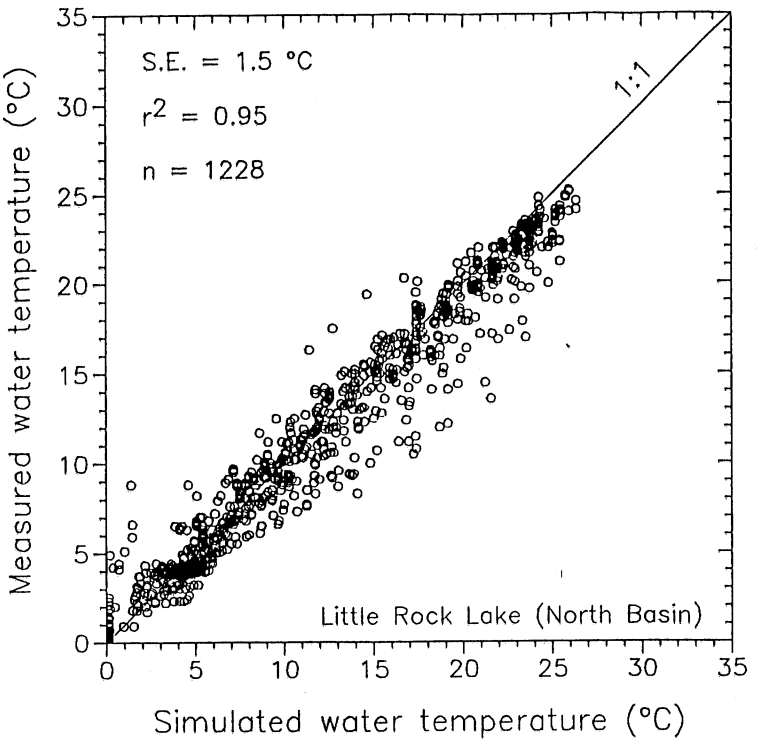

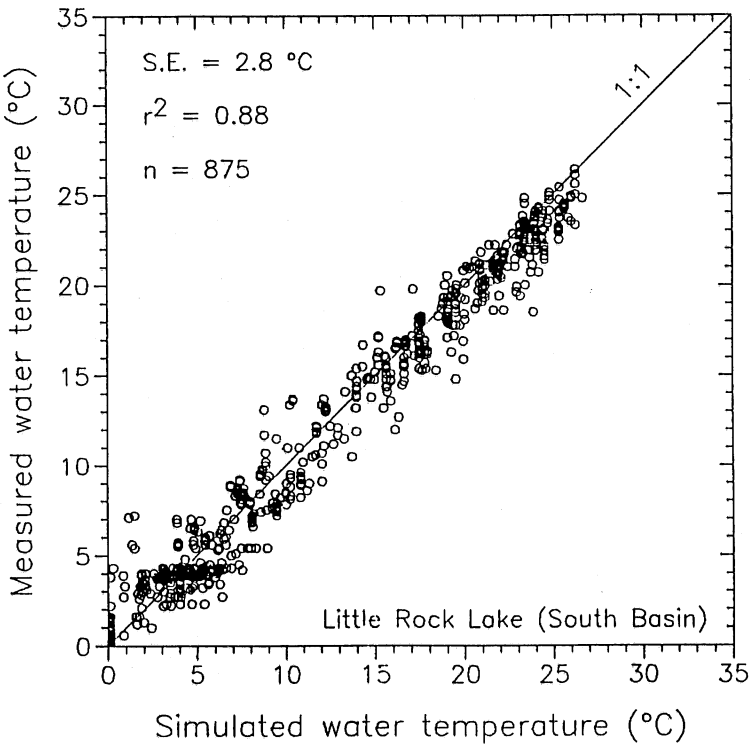

Fig. 19. Simulated and measured water temperatures in both north and south basins of Little Rock Lake at all depths from 1983 to 1991.

Table 4. Statistics of errors between simulated and measured water temperatures in Little Rock Lake, Wisconsin.

South Basin			North Basin		
Depths	Regression Coefficient	Standard Error (°C)	Depths	Regression Coefficient	Standard Errors (°C)
All	0.97	1.41	All	0.95	1.51
Summer	0.95	1.45	Summer	0.92	1.66
Winter	NA	1.29	Winter	0.20	1.00
z=1 m	0.98	1.26	z=1 m	0.98	1.21
z=3 m	0.98	1.06	z=3 m	0.98	1.06
z=4 m	0.97	1.30	z=5 m	0.95	1.61
z=5 m	0.95	1.64	z=8 m	0.81	1.58
z=6 m	0.93	1.78	z=9 m	0.77	1.35

5. WINTER DISSOLVED OXYGEN MODEL DEVELOPMENT

5.1 Governing Equations

The winter dissolved oxygen (D.O.) model formulation is guided by a one-dimensional dissolved oxygen model for the open water season developed by Fang and Stefan (1994) (see Fig. 20). This D.O. model was previously applied to 27 classes of Minnesota lakes for both past climate conditions and a projected future climate scenario ($2xCO_2$ GISS model).

The one-dimensional, deterministic, unsteady D.O. transport equation was given as (Fang and Stefan, 1994)

$$\frac{\partial C}{\partial t} = \frac{1}{A}\frac{\partial}{\partial A}\left(A\,K_Z\frac{\partial C}{\partial z}\right) - \frac{S_b}{A}\frac{\partial A}{\partial z} + P_{max}\,Min[L]\,Chla$$
$$- \frac{1}{YCHO2}\,k_r\,\theta_r^{T-20}\,Chla - k_b\,\theta_b^{T-20}\,BOD \qquad (14)$$

where C(z,t) is the dissolved oxygen concentration in mg L^{-1} as a function of depth (z) and time (t), A(z) is the horizontal area in m^2, K_Z is the turbulent diffusion coefficient in m^2 day^{-1}, S_b is the sedimentary oxygen demand coefficient in mg O_2 (m^{-2} day^{-1}), P_{max} is the maximum specific oxygen production rate by photosynthesis at saturating light conditions in [mg O_2 (mg Chla)$^{-1}$ hr^{-1}], Min[L] is the light limitation determined by the Haldane equation, Chla is the chlorophyll-a concentration in mg L^{-1}, YCHO2 is the yield coefficient which is the ratio of mg chlorophyll-a to mg oxygen, k_r and k_b are the first order decay for BOD and respiration rate coefficient (day^{-1}), respectively, θ_r and θ_b are the temperature adjustment coefficient for plant respiration and BOD, BOD is the biochemical oxygen demand concentration in mg L^{-1}, and T(z,t) is the water temperatures in °C. In the model, the surface gas transfer (reaeration), $k_e\,(C_s - C) / \Delta Z_s$, is the oxygen resource or sink term in the topmost water (surface) layer, and diffusive oxygen flux at the lake bottom is zero as a boundary condition (SOD is an active sink at the lake bottom). For the dissolved oxygen simulations in a lake with ice cover, modifications must be made in eq. (14)

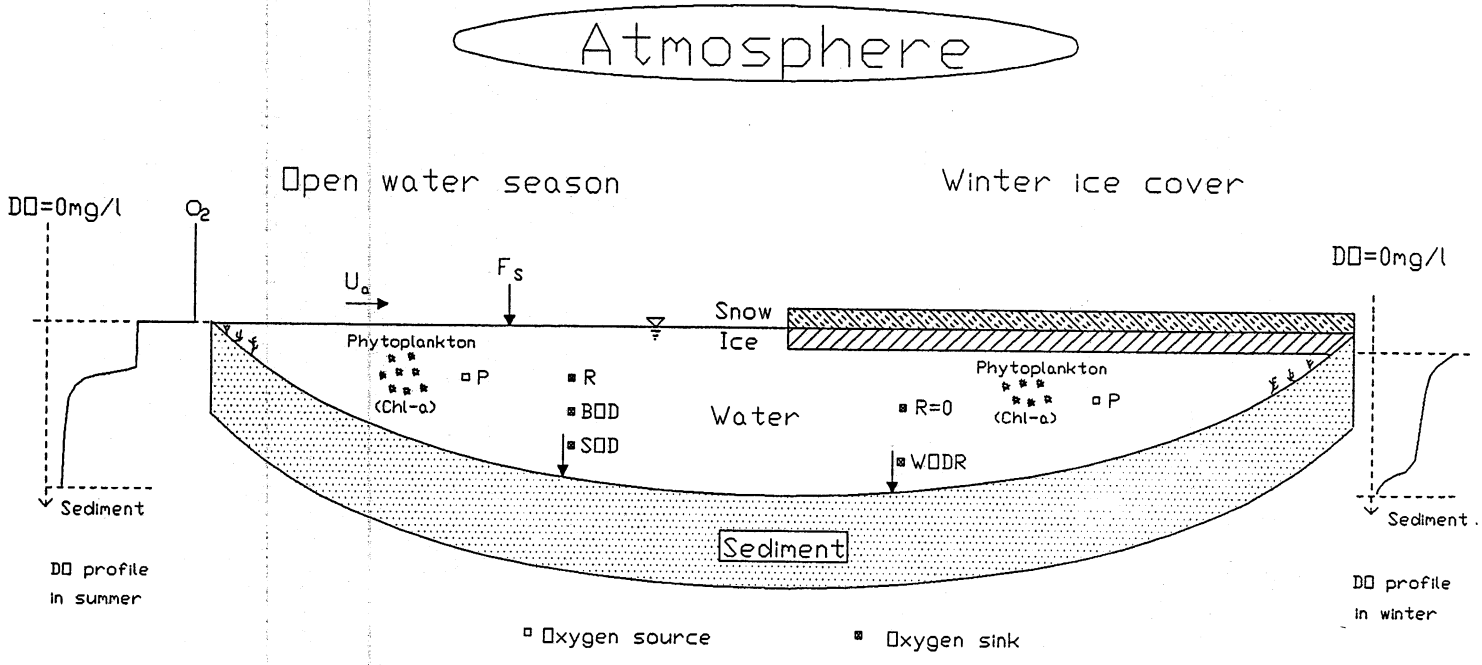

Fig. 20. Schematic representation of source and sink terms in the lake dissolved oxygen model in summer and winter.

to account for the presence of an ice cover and low temperatures over the winter season. These modifications will be discussed below.

5.2 Photosynthesis and Surface Gas Transfer

Photosynthetic oxygen production, $P = P_{max}$ MIN[L] Chla, becomes more difficult to evaluate during the winter. Available active irradiance below the ice-cover can be very small due to the attenuation of snow cover and ice cover or quite substantial when the ice is transparent and snow cover is absent. The snow and ice thicknesses simulated by the water temperature model significantly affect under-water irradiance, and therefore oxygen production by photosynthesis, and hence the total oxygen content in an ice-covered lake, especially in lakes with clear ice without snow cover (Ellis and Stefan, 1990). In this study lack of data did not permit further improvement of the photosynthetic oxygen production simulation. Therefore formulas for determining P_{max} and MIN[L] in the open water season (summer) are used in the winter D.O. model, but photosynthesis in winter is smaller than in summer because of attenuation of light through snow/ice and low temperature effects (P_{max} and MIN[L] are temperature dependent).

The ice cover on a lake also prevents any significant gas exchange between atmosphere and water, i.e. reaeration is zero. Therefore the bulk surface gas transfer coefficient, k_e, is set equal to zero in the winter D.O. model.

5.3 Water Column Oxygen Demand

5.3.1 Plant respiration

Much of a lake's phytoplankton die in the fall, and hence chlorophyll-a concentrations in winter are fairly small (Hutchinson, 1957). The respiration rate coefficient (k_r) is also very low at the low water temperatures (0°C to near 4°C) encountered during the winter. Oxygen consumption by plant respiration therefore becomes very small and is not presented as a separate sink term in the winter D.O. model ($k_r = 0.0$). Instead it is included into water column oxygen demand (WOD) given, e.g. by Ellis and Stefan (1989) and Stefan (1990).

5.3.2 Biochemical oxygen demand

Many field studies of oxygen demand in ice-covered lakes have been performed because of winterkill of fishes (Barica and Mathias, 1979; Mathias and Barica, 1980; Charlton, 1980; Babin and Prepas, 1985; Ellis and Stefan, 1989). Mathias and Barica (1980) used four sets of Canadian lakes (Prairie, southeastern Ontario, Arctic, and

Experimental Lake Area) with different lake morphometries and trophic states to determine volumetric winter oxygen depletion rate (V_{WODR} in g O_2 m^{-3} day^{-1}):

$$\text{Eutrophic Lakes:} \quad V_{WODR} = 0.226 \frac{A_{SED}}{V} + 0.010$$

$$\text{Oligotrophic Lakes:} \quad V_{WODR} = 0.075 \frac{A_{SED}}{V} + 0.012 \tag{15}$$

where A_{SED} (m^2) is the surface area of sediment and V (m^3) is the total volume of a lake. In equation (15), the coefficient before A_{SED}/V is representative of the oxygen demand of a unit area of sediment (S_b in g O_2 m^{-2} day^{-1}), whereas the constant is representative of the oxygen demand of the water column above the sediment (WOD in g O_2 m^{-3} day^{-1}). WOD is mainly composed of biochemical oxygen demand (BOD) due to detritus in suspension and including bacterial respiration, and plant respiration (Stefan, 1990). Because A_{SED} is approximately equal to lake surface area A_S, therefore A_{SED}/V can be rewritten as $1/Z_m$, where Z_m is the mean depth of a lake and defined as V/A_S (Hutchinson, 1957). Therefore the winter oxygen depletion rate (WODR) can be expressed on a per unit surface area basis and thus has units of (g O_2 m^{-2} day^{-1}) (Barica and Mathias, 1979; Ellis and Stefan, 1989):

$$WODR = S_b + WOD * Z_m \tag{16}$$

Charlton (1980) related WODR to mean chlorophyll-a concentrations and mean hypolimnetic thicknesses.

Equation (15) developed by Mathias and Barica (1980) is only one formula in which lakes were classified in terms of trophic state (based on mean summer chlorophyll-a concentration). Equation (15) is used in the winter D.O. model. Because the difference between 0.010 and 0.012 in Eqn. (15) is probably within the measurement errors, water column oxygen demand, WOD, was set as a constant (0.010 g O_2 m^{-3} day^{-1}) for eutrophic, mesotrophic and oligotrophic lakes (Mathias and Barica, 1980).

5.3.3 Sediment oxygen demand

Sedimentary oxygen demand coefficient (S_b) is dependent on trophic state, and was set equal to 0.226, 0.152, and 0.075 (g O_2 m^{-2} day^{-1}) for eutrophic, mesotrophic, and oligotrophic lakes, respectively. The values for eutrophic and oligotrophic lakes were obtained from equation (15), and the value for mesotrophic lake is the average of above two values. They will be calibrated against measurements from different lakes with ice cover.

6. DISSOLVED OXYGEN SIMULATIONS

The winter D.O. model calibrations were performed for Thrush Lake, MN, and Little Rock Lake, WI. Both lakes are small transparent, oligotrophic lakes. Ultimate biochemical oxygen demand (BOD) was set at 0.5 mg L^{-1} for both lakes over the entire simulation period. Measured chlorophyll-a concentrations are model input; daily chlorophyll-a concentrations were calculated by a step function in which chlorophyll-a value is the average of the two nearest field data points. The parameters and coefficients used in the dissolved oxygen model simulations for the open water season were given in detail by Fang and Stefan (1994), and are summarized in Table 5. The initial condition of the dissolved oxygen simulations is a uniform D.O. profile with a concentration of 10 mg L^{-1}. The simulation in Thrush Lake was for the period from April 16, 1986, to October 31, 1992 (6 years).

Fig. 21 shows simulated dissolved oxygen profiles in **Thrush Lake** during the winter of 1986. Dissolved oxygen concentrations are near or over saturation near the ice-water interface, and slowly decrease with depth, approaching zero (anoxic conditions) at the lake bottom. The simulations fit measurements well near the lake bottom, and underestimate measurements in the surface region just below the ice-water interface, e.g. on March 17, 1987 when ice is clear and without snow cover.

Fig. 22 shows time-series plots of simulated and measured dissolved oxygen concentrations in Thrush Lake from 1986 to 1991. The model simulates surface D.O. well in the open water season. The seasonal distributions of D.O. concentrations in the hypolimnion show that the model has difficulty to predict spring overturns in Thrush Lake. After a long winter with ice-cover the D.O. concentrations are usually very low (near anoxic conditions) near the lake bottom. Spring overturn can bring the D.O. concentrations up to saturated values rapidly (10 - 13 mg L^{-1}). If the model simulation missed the spring overturn, the D.O. at the lake bottom stays low as shown in Fig. 22, especially for the spring of 1990 and 1991.

Standard errors between simulated and measured D.O. concentrations are 2.31, 2.28 and 2.29 mg L^{-1} for the ice-cover periods, the open water seasons and the total simulation periods (indicated as Winter, Summer and All in Table 2), respectively. **Errors during the winter periods** are mainly due to: (1) photosynthetic oxygen production (e.g. underestimated in the winters of 1986-87 and 1989-90, but overestimated in the winters of 1987-88 and 1988-89, Figs. 21 and 22); (2) variations in sedimentary oxygen demand from year to year (e.g. underestimated in the winters

Table 5. Parameter and coefficient values in the D.O. model

Coefficients		Open Water Season	Ice-cover Period
K_b (day^{-1})		0.10	0.03
θ_b		1.047	1.0[a]
k_r (day^{-1})		0.10	0.0
θ_r		1.047	1.0[a]
K_e ($m\ day^{-1}$)		f(T, Wind)	0.0
YCHO2		0.0083	0.0083
θ_p		1.036	1.036
θ_s		1.065	1.0[a]
k_b ($g\ O_2\ m^{-2}\ day^{-1}$)	Eutrophic	1.0 - 2.0[b]	0.23
	Mesotrophic	0.5 - 1.0[b]	0.16
	Oligotrophic	0.2 - 0.5[b]	0.08

Note: [a] - Rate coefficients for BOD, SOD and respiration are independent of temperature; [b] - values are dependent on the maximum depth of a lake.

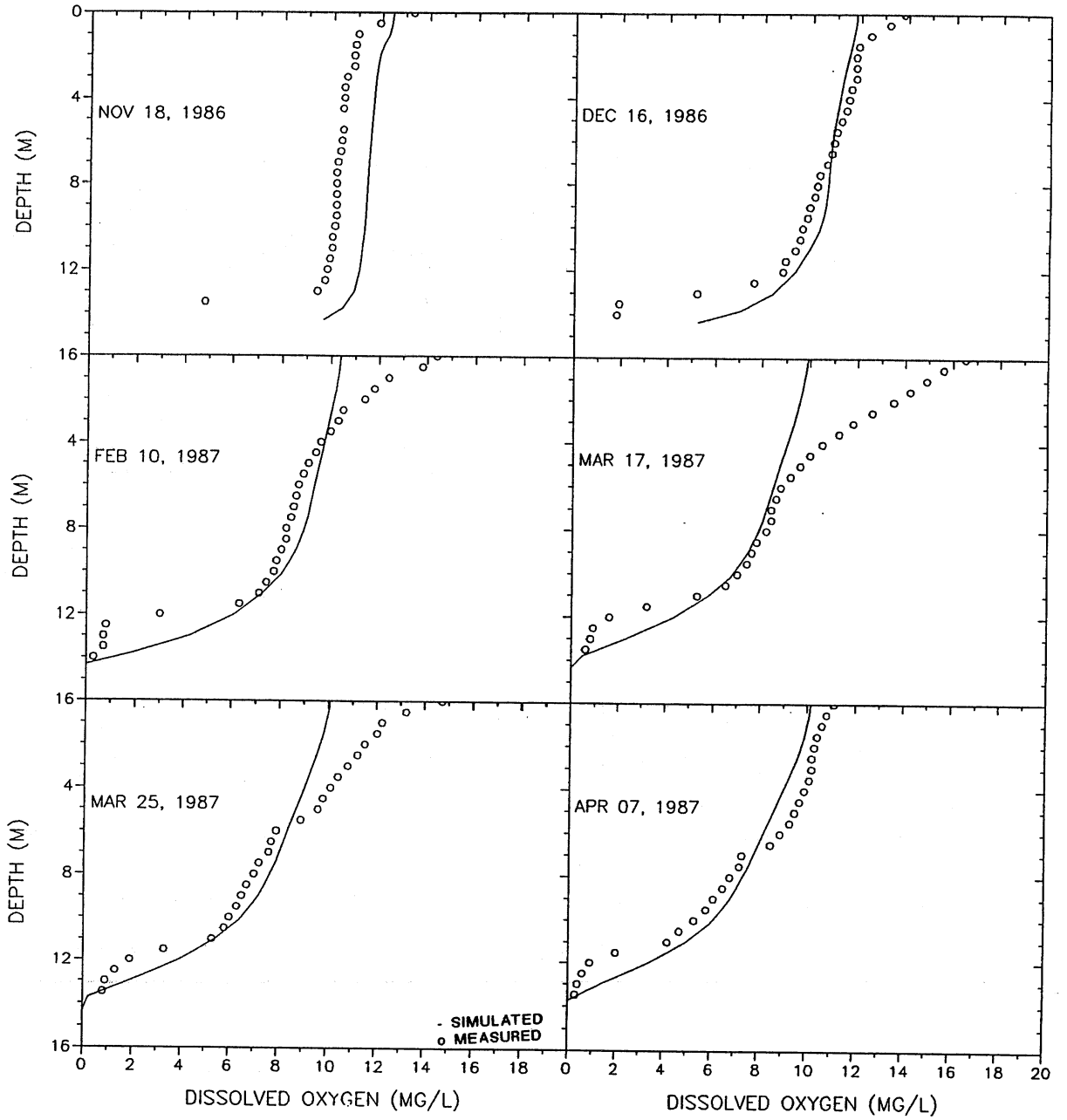

Fig. 21. Simulated and measured dissolved oxygen profiles in Thrush Lake, Minnesota, during the ice cover period of year 1986.

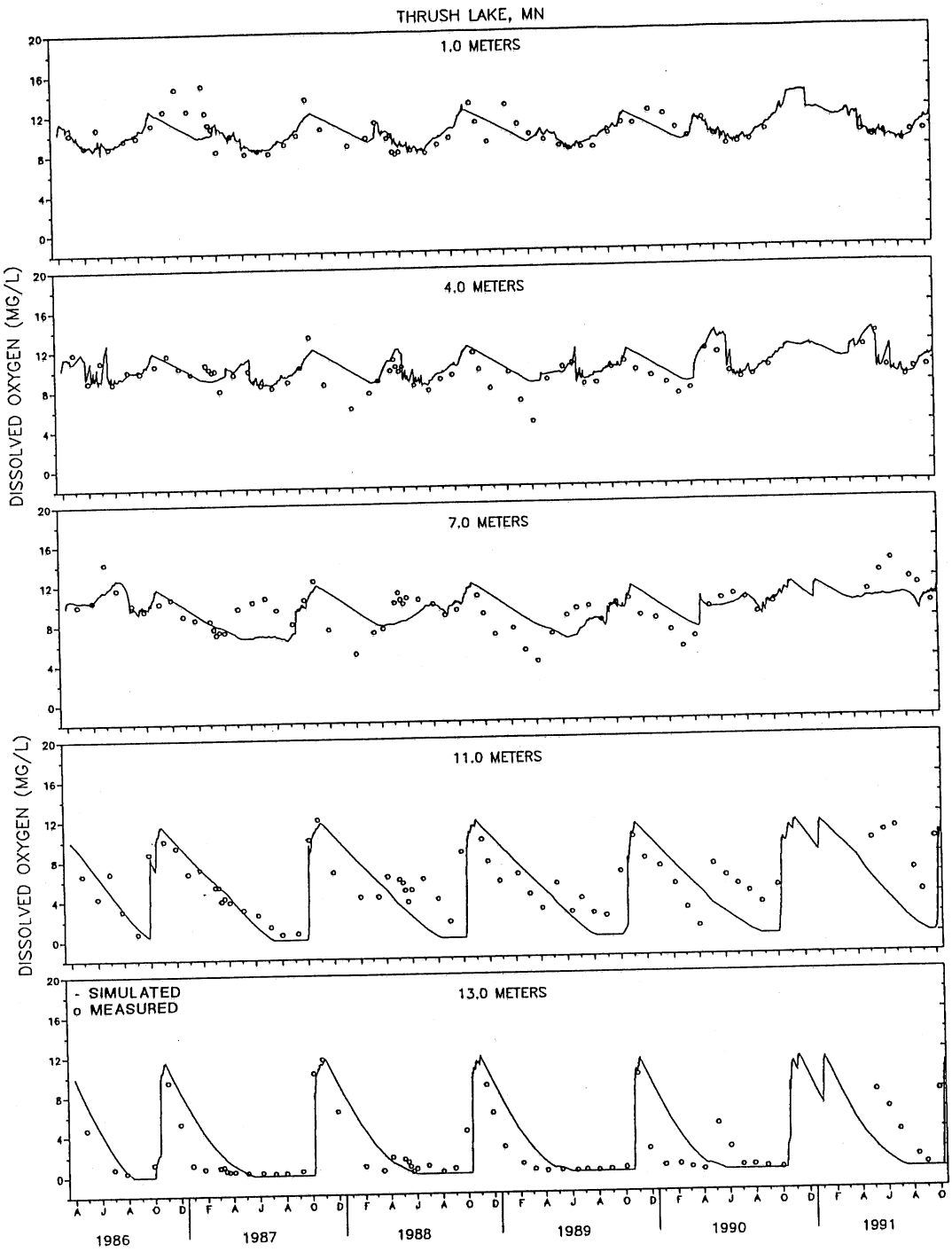

Fig. 22. Time-series plot (1986-1992) of simulated and measured dissolved oxygen concentrations in Thrush Lake, Minnesota.

of 1987-88 and 1988-89, Fig. 22). **Errors during the open water seasons** are mainly due to: (1) missing of the spring overturns in the water temperature simulation of Thrush Lake (Fig. 22); (2) underestimated metalimnetic oxygen maxima (see time-series plot at 7 meters in Fig. 22).

Fig. 23a and 23b show time-series plots of simulated and measured dissolved oxygen concentrations in the south basin and the north basin of **Little Rock Lake**, respectively. Statistical results of errors between simulated and measured dissolved oxygen concentrations are given in Table 6. Standard errors during the winter period in both basins are larger than those in the open water season. The model overestimated D.O. concentrations in the region below the ice-water interface for most of the years (see time-series plots at 1, 3 and 4 meters in Fig. 23). During the open season the model missed some of the spring overturns again, especially in the deep north basin (Fig. 23b).

Both Thrush Lake and Little Rock Lake are small, oligotrophic lakes with metalimnetic oxygen maxima during the open water season, which are usually more difficult to simulate than medium size eutrophic lakes. Metalimnetic oxygen maxima can be simulated by the model at about the correct depth but are not always of correct magnitude which is associated with specification of chlorophyll-a concentration below the metalimnion (Fang and Stefan, 1994).

Photosynthesis under the ice cover depends strongly on the correct simulation of snow thicknesses in the range from 0 to 5 cm. This is fairly difficult to accomplish.

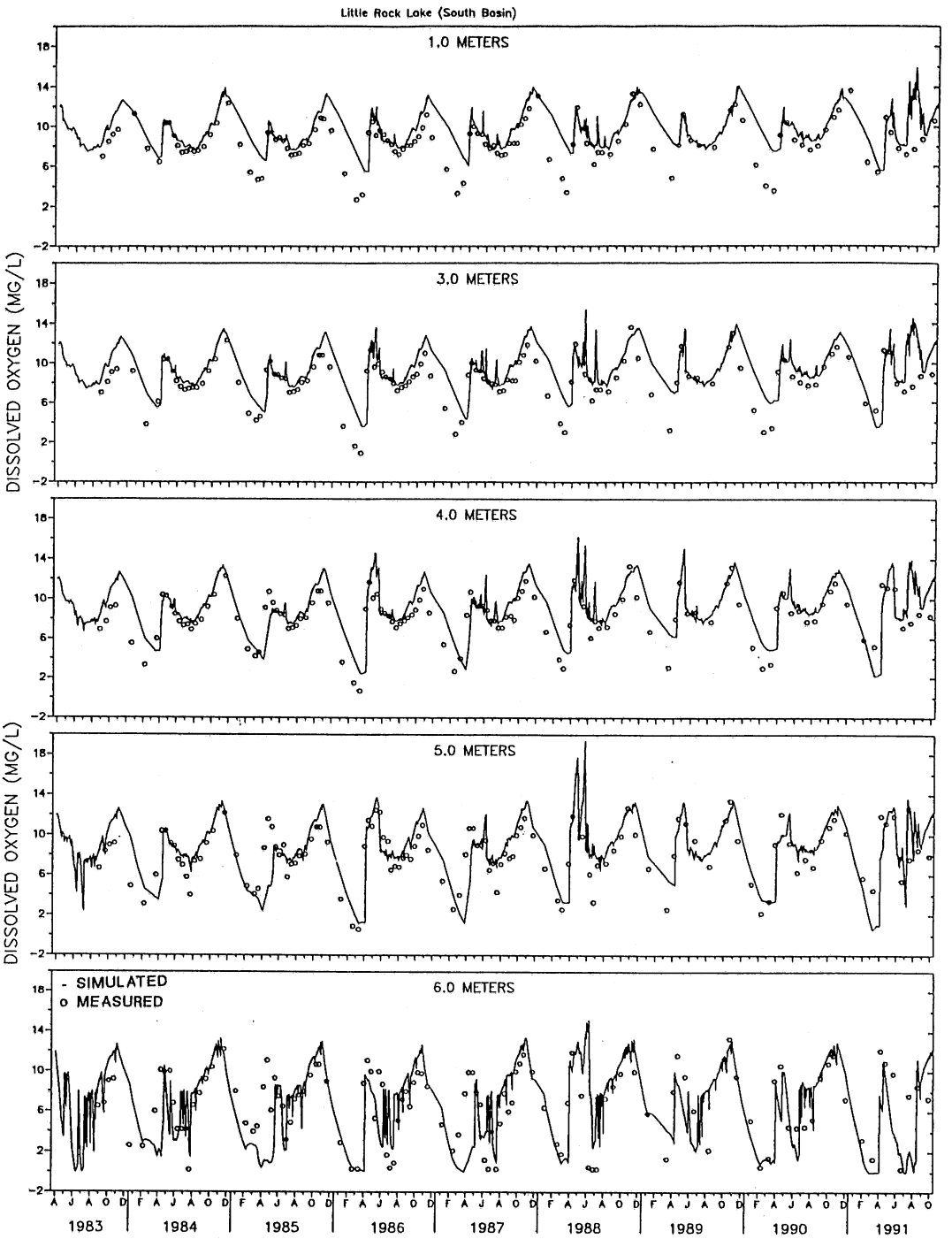

Fig. 23a. Time-series plot (1983-1991) of simulated and measured dissolved oxygen concentrations in the south basin of Little Rock Lake, Wisconsin.

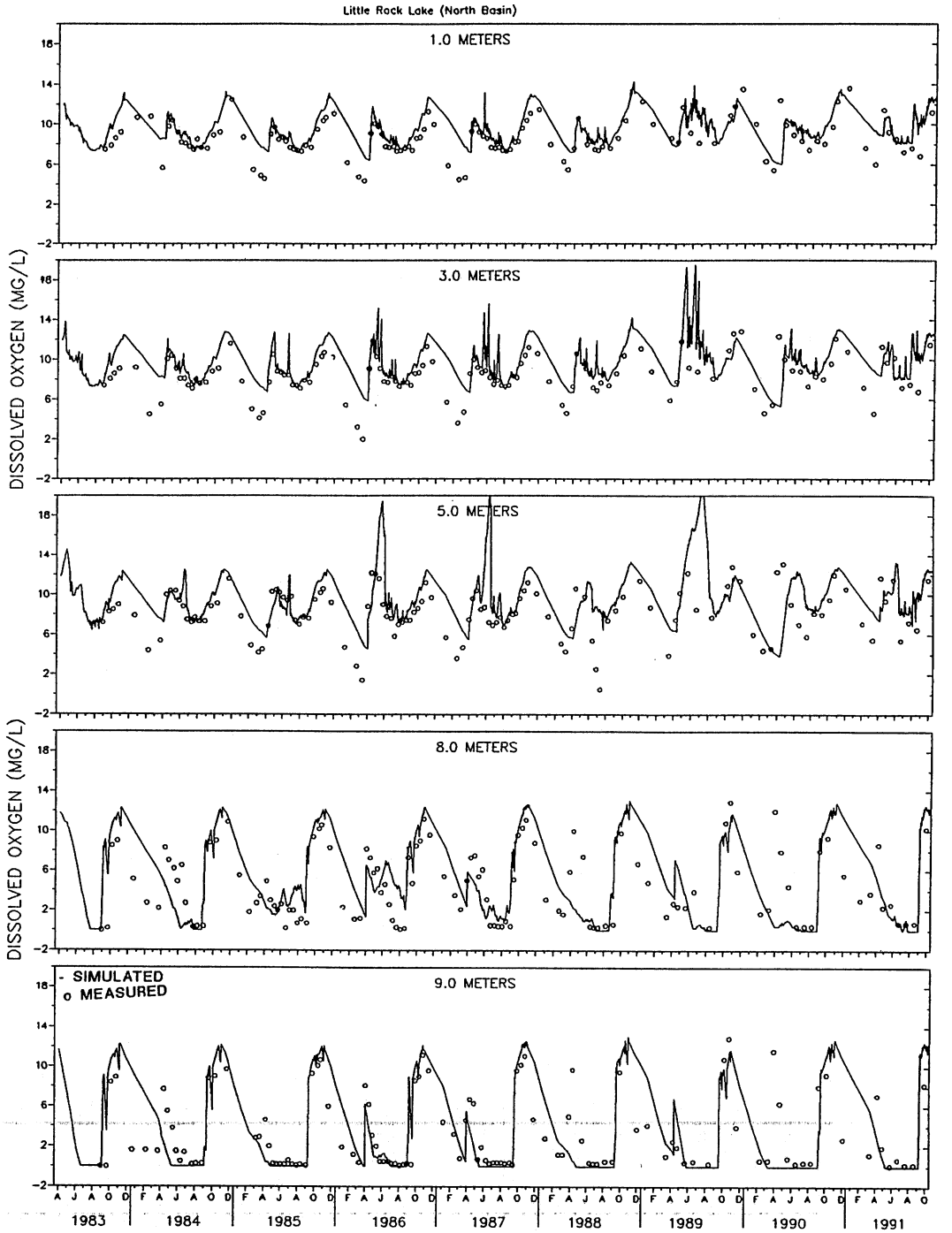

Fig. 23b. Time-series plot (1983-1991) of simulated and measured dissolved oxygen concentrations in the north basin of Little Rock Lake, Wisconsin.

Table 6. Statistics of errors between simulated and measured dissolved oxygen concentrations in Little Rock Lake, Wisconsin.

South Basin			North Basin		
Depths	Regression Coefficient	Standard Error (mg L^{-1})	Depths	Regression Coefficient	Standard Error (mg L^{-1})
All	0.25	2.27	All	0.36	2.57
Summer	NA	2.17	Summer	0.43	2.36
Winter	0.42	2.55	Winter	0.15	3.10
z=1 m	0.27	1.94	z=1 m	0.37	1.59
z=3 m	0.37	1.93	z=3 m	0.09	2.05
z=4 m	0.41	1.92	z=5 m	NA	2.83
z=5 m	0.34	2.29	z=8 m	0.29	3.03
z=6 m	NA	3.60	z=9 m	0.42	2.86

7. CONCLUSIONS

(1) A water temperature model (Gu and Stefan, 1990) for lakes with ice cover has been substantially modified to simulate water temperature structures over many years for three lakes. Vertical diffusion coefficients determined by Ellis et al.(1990, 1994) based on water temperature measurements in Ryan Lake, MN, have been used in the model. Sediment heat flux has been included for all layers from the water surface to the lake bottom. A modified computational scheme has been incorporated in the model.

(2) The modified winter water temperature simulation model was calibrated for Thrush Lake, MN, and further validated for Ryan Lake, MN, and Little Rock Lake, WI. The simulations were started on April 16 of the first year for which data were available and ended on October 31 of the most recent year for which measurements were available. Model parameters/coefficients are kept constant over the entire simulation period. Standard errors between simulations and measurements for the open water season, the ice-cover period and whole simulation period, e.g. in Thrush Lake from 1986 to 1991, were 1.37, 0.48, 1.07 °C, respectively.

(3) A sensitivity analysis on a threshold condition for ice formation was performed. The threshold condition T_{mean} is dependent on both lake morphometry and weather data used in the simulation. The best value of T_{mean} for Thrush Lake is 3.3 °C.

(4) A winter dissolved oxygen model in a lake with ice cover has been developed. Photosynthetic oxygen production is the source term, and water column (biochemical) oxygen demand (WODR) and sedimentary oxygen demand are the sink terms for the winter dissolved oxygen model. Surface gas transfer is eliminated by the ice cover, and plant respiration is joint with WODR.

(5) The winter dissolved oxygen model was applied to Thrush Lake, MN, and Little Rock Lake, WI (both south and north basin). The standard errors during ice-cover periods were 2.28, 2.55, and 3.1 mg L^{-1} for Thrush Lake, south basin and north basin of Little Rock Lake, respectively. Reasons for these large errors have been analyzed and recommendations for further lines of investigation will be made in the following section.

8. RECOMMENDATIONS

The temperature model simulates the water temperature structures during the winter and the open water season quite well. Further improvement of the model requires further study in the following areas:

(1) Ice formation in the model is dependent on three threshold conditions: air temperature < -2 °C; wind speed < 5 m s^{-1}; mean volumetric averaged temperature T_{mean} < 3.3°C, 2.5°C for Thrush Lake and Little Rock Lake, respectively. Threshold conditions for ice formation should be and can be eliminated for regional lake study if we reexamine the full heat budget and wind/convective mixing in the fall.

(2) The snow compacting coefficient ranges from 0.2 to 0.4 (Adams, 1981), and can greatly affect cumulative snow thicknesses in the winter model, and thereby influences ice thicknesses and water temperatures. More study of the snow compaction process is warranted.

(3) It seems that the model could not successfully simulate all spring overturns. This does not significantly affect the water temperature stratification in summer but influences the dissolved oxygen concentrations at the lake bottom. Mixing mechanics in spring need to be reexamined, e.g. increase the wind sheltering coefficient due to lack of leaves on trees around a lake in spring, and force convective mixing when surface water temperatures change from below to above 4 °C (point of maximum water density) after the ice-out. Daily timestep may be too long.

(4) Sediment heat diffusion coefficients (K_s) vary from lake to lake, which affects prediction of water temperatures (especially near the lake bottom) during the winter. For individual lakes, more information regarding the composition of sediments is useful to estimate K_s. For regional lake simulations, to specify K_s dependent on eutrophic status may not be a bad choice, since sediments in a eutrophic lake usually contain more organic material than in an oligotrophic lake.

The dissolved oxygen model is a good basis for further development and improvement. Recommendations are as follows:

(1) Better estimation of photosynthetic oxygen production during the winter is essential for the improvement of the winter D.O. model. This is a very difficult task also. More basic research is needed.

(2) Chlorophyll-a concentrations greatly affect photosynthetic oxygen production, especially below the metalimnion of an oligotrophic lake. "Averaged" epilimnetic and hypolimnetic chlorophyll-a concentrations were used in the D.O. model. Limited measured chlorophyll-a concentrations with depth were used to determine those averages. Because great variations of chlorophyll-a concentrations occur in the hypolimnion (Fee, 1976), it is unlikely that a few measurements with depth are representative of the average hypolimnetic chlorophyll-a concentration. It therefore may be necessary to use a model (i.e. Riley and Stefan, 1987) or to develop a model to simulate chlorophyll-a concentration profiles with depth.

(3) Inclusion of oxygen production and consumption by macrophytes may be needed.

(4) The study of sediment oxygen demand in lakes both for the open water season and the winter ice-cover period are very necessary and important.

(5) The winter dissolved oxygen model was calibrated in two small, wind sheltered, oligotrophic lakes for which winter dissolved oxygen measurements were available. It is necessary to calibrate the model in larger and eutrophic lakes if winter data can be found, which will help to identify problems more clearly.

REFERENCES

Adams, W.P., 1981. Snow and ice on lake, In: D.M. Gary and D.H. Male (Editors), Handbook of snow. Pergamon Press, Oxford, Ch. 10.

Ashton, G.D., 1980. Freshwater ice growth, motion, and decay. In Dynamics of Snow and Ice Masses by S.C. Colbeck (editor). Academic Press, Inc., New York, pp. 261-304.

Ashton, G.D., 1986. River and Lake Ice Engineering. Water Resources Publications, Littleton, Colo.

Babin, J., and Prepas, E.E., 1985. Modelling winter oxygen depletion rates in ice-covered temperate zone lakes in Canada. Can. J. Fish. Aquat. Sci. 42:239-249.

Barica, J., and Mathias, J.A., 1979. Oxygen depletion and winterkill risk in small Praire lakes under extended ice cover. J. Fish. Res. Board Can. 36:980-986.

Blumberg, A.F., and DiToro, D.M., 1990. Effects of climate warming on dissolved oxygen concentrations in Lake Erie. Transactions of the American Fisheries Society, 119(2), 210-223.

Brezonik, P.L., Baker, L., Detenbeck, N., Eaton, J., Frost, T., Garrison, P., Johnson, M., Kratz, T., Magnuson, J., McCormick, J., Perry, J., Rose, W., Shephard, B., Swenson, W., Watras, C., Webster, K., 1985. Experimental acidification of Little Rock Lake, Wisconsin, Baseline studies and predictions of lake responses to acidification. Water Resources Research Central, University of Minnesota, St. Paul, Special Rep. No. 7.

Charlton, M.N., 1980. Hypolimnion oxygen consumption in lakes: Discussion of productivity and morphometry effects. Can J. Fish. Aquat. Sci. 37:1531-1539.

DiToro, D. M., and Connolly, J. P., 1980. Mathematical models of water quality in large lakes, Part 2: lake Erie, U.S. Environmental Protection Agency, Environmental Research Laboratory, Duluth, Minnesota, EPA-600/3-80-065.

Ellis, C.R., and Stefan, H.G., 1989. Oxygen demand in ice-covered lakes as it pertains to winter aeration. Water Resources Bulletin, American Water Resources Association, Vol. 25(6).

Ellis, C.R., Stefan, H.G. and Gu, R., 1991. Water temperature dynamics and heat transfer beneath the ice cover of a lake. Limnol. Oceanogr., 36(2): 324-335.

Ellis, C.R., and Stefan, H.G., 1994. Density current intrusions and vertical eddy

diffusivity in an ice-covered lake. Submitted for publication in Limnology and Oceanography.

Fang, X. and Stefan, H.G., 1994. Modeling of dissolved oxygen stratification dynamics in Minnesota lakes under different climate scenarios. Project report No. 339, St. Anthony Falls Hydraulic Laboratory, University of Minnesota, Minneapolis, MN 55414.

Fertuck, L.J, Spyker, J.W., and Husband, W.H.W., 1971. Numerical estimation of ice growth as a function of air temperature, wind speed and snow cover. Tans. Can Soc. Mech. Eng., EIC, B-9, p.14.

Fee, E.J., 1976. The vertical and seasonal distribution of chlorophyll in lakes of in the Experimental Lakes Area, northwestern Ontario, implication for primary production. Limnology and Oceanography, 21, 767-783.

Ford, D.E. and Stefan, H.G., 1980. Thermal predictions using integral energy model. J. Hydraulic Div., ASCE, 106(1): 39-55.

Gu, R. and Stefan, H.G., 1993. Validation of cold climate lake temperature simulation. Cold Reg. Sci. Technol., 22: 99-104.

Gu, R. and Stefan, H.G., 1990. Year-round temperature simulation of cold climate lakes. Cold Reg. Sci. Technol., 18(2): 147-160.

Gu, R. and Stefan, H.G., 1991. Numerical simulation of stratification dynamics in the Harris wastewater stabilization ponds. Project report 309, St. Anthony Falls Hydraulic Laboratory, University of Minnesota, Minnesota 55414.

Harleman, D.R.F., 1986. Hydrothermal modeling of reservoirs in cold regions: status and research needs. Proc. Cold Reg. Hydrol. Symp., AWRA, pp. 39-49.

Hondzo, M. and Stefan, H.G., 1993. Lake water temperature simulation model. J. Hydraulic Eng., ASCE, 119(11): 1251-1273.

Hutchinson, G.E., 1957. A Treatise On Limnology. Vol.2, Wiley, New York.

Light, P., 1941. Analysis of high rates of snow-melting, Reports and papers, Snow-survey conference, Transactions, American Geophysical Union.

Jassby, A., and Powell, T., 1975. Vertical patterns of Eddy diffusion during stratification in Castle Lake, california. Limnology and Oceanography, 20(4), 530-543.

Mathias, J.A., and Barica, J., 1980. Factors controlling oxygen depletion in ice-covered lakes. Can J. Fish. Aq. Sci. 37:185-194.

Michel, B., 1971. Winter regimes of rivers and lakes. U.S. Army Cold Reg. Res. Eng. Lab., Hanover, N.H. Monogr. 3-Bla.

Mortimer, C.H., 1942. The exchange of dissolved substances between mud and water in lakes. Journal of Ecology, 30, 147-201.

Patterson, J. C., Hamblin, P. F., 1988. Thermal simulation of a lake with winter ice cover. Limnol. Oceanogr., 33(3): 323-338.

Pivovarov, A.A., 1972. Thermal Condition in Freezing Lakes and Rivers. Wiley, New York, New York.

Riley, M.J., and Stefan, H.G., 1987. Dynamic lake water quality simulation model "MINLAKAE". Project report No. 264, St. Anthony Falls Hydraulic Laboratory, University of Minnesota, Minneapolis, MN, 55414.

Sampson, C.J., 1992. Chemical responses in experimentally acidified Little Rock Lake, Wisconsin. Master Thesis, Graduate School of the University of Minnesota, Minneapolis, MN.

Stefan, H.G., 1990. Sediment oxygen demand and its effects on winterkill in lakes. *In* Proceeding of US Army Corps of Engineers workshop on sediment oxygen demand; (Editors: Cerco, C., Gunnison, D., and Price, C.B.), Providence, Rhode Island, 21-22, August, 1990. Miscellaneous paper W-92-1, Vicksburg, MS, 1986pp.

Stefan, H.G., Hondzo, M., Sinokrot, B., Fang, X., Eaton, J.G., Goodno, B., Hokanson, K., McCormick, J.H., O'Brien, D., and Wisniewski, J., 1992. A methodology to estimate global climate change impact on lake and stream environmental conditions and fishery resources with application to Minnesota. Projects report 323, St. Anthony Falls Hydraulic Laboratory. University of Minnesota, Minneapolis, Minnesota.

Stefan, H.G., Hondzo, M., Fang, X., 1993. Lake water quality modeling for projected future climate scenarios. Journal of Environmental Quality, Vol. 22(3). 417-431.

Stefan, H.G., Hondzo, M., Fang, X., and Rasmussen, A.H., 1994. Year-round water temperature and dissolved oxygen model for lakes with winter ice cover. Project report No. 355, St. Anthony Falls Hydraulic Laboratory, University of Minnesota, Minneapolis, MN 55414.

Tsay, T.K., Ruggaber, G.J., Effler, S.W., and Driscoll, C.T., 1992. Thermal stratification modeling of lake with sediment heat flux. Journal of Hydraulic Engineering, ASCE, 118(3), 407-419.

Wellander, P., 1967. Theoretical forms for the vertical exchange coefficients in a stratified fluid with application to lakes and seas. ACTA Regiae Societatis Scientarum et Litterarum, Gothoburgensis, Geophysical, 27.

Williams, G.P., 1969. Water temperature during the melting of lake ice. Water Resources Research, 5(5): 1134-1138.

Wright, D., 1993. Unpublished measurements of snow and ice thickness (Personnel communication), Department of Natural Resources, St. Paul, MN.

Wright, D., Lawrenz, R., Popp, W. and Danks, M., 1989. Acid precipitation mitigation program, Thrush Lake, Cook County Program - Annual report fiscal year 1988. Department of Natural Resources, St. paul, MN. 182pp.

Appendices

Appendix A. Snow Thickness Prediction in the Winter Temperature Model

Snow accumulation due to precipitation accompanied by a compaction process, melting on the snow surface due to conduction or convection, rainfall, long wave radiation, and melting in the snow layer due to absorption of short wave radiation are the processes which are taken into account in order to determine the snow thickness. The snow cover forming on the ice surface of a lake is likely to be thinner than direct accumulations of snowfall, therefore a snow compacting factor (0.2 - 0.4), C_{sw}, is used before adding snowfall to the existing snow depth (Adams, 1981; Gu and Stefan, 1990). The change in snow thickness over one day is given by a mass balance equation

$$\frac{dz_{sw}}{dt} = C_{sw} P_{sw} - \dot{z}_s - \dot{z}_e - \dot{z}_c - \dot{z}_r \qquad (17)$$

where z_{sw} is the snow thickness (m), P_{sw} is the snow fall from given weather date (m day^{-1}), $\dot{z}_s$, $\dot{z}_e$, $\dot{z}_c$ and $\dot{z}_r$ are the snow depth reduction rates by melting (m day^{-1}) due to the solar radiation, convection heat transfer, evaporation, and rainfall, respectively. In the model, snow melting only occurs as if air temperature (T_a) is larger than zero.

The snow melting on the snow surface or within the snow due to solar radiation is determined by the energy balance equation (Gu and Stefan, 1990)

$$\dot{z}_s = \frac{H_{sw}}{\rho_{sw} \lambda_{sw}} \qquad (18)$$

where ρ_{sw} is the snow density (kg m^{-3}), λ_{sw} is the latent heat of fusion of snow (kcal kg^{-1}), and H_{sw} is the solar radiation flux (kcal m^{-2} day^{-1}) absorbed in the snow layer given by

$$H_{sw} = H_s \{\beta_{sw} + (1 - \beta_{sw})(1 - \alpha_{sw})[1 - \exp[(-\mu_{sw} z_{sw})]\} \qquad (19)$$

where H_s is the incoming solar radiation on the snow surface, β_{sw} is the surface absorption coefficient for snow, α_{sw} is the surface reflectivity for snow, μ_{sw} is the attenuation coefficient in snow.

The snow depth reduction rate, $\dot{z}_c$ (m day^{-1}), due to the convective heat transport rate H_c, was given by Light (1941)

$$\dot{z}_c = 0.000376\ 10^{-0.0000156 Z_w}\ U_a\ (T_a - 32) \qquad \text{for } T_a > 0^{\circ}C \tag{20}$$

where z_w is the weather station-elevation (ft) above the mean sea level, U_a and T_a are the wind speed (m sec^{-1}) and air temperature (°F) at the 10 ft above the snow surface, respectively. Coefficient 3.76×10^{-4} in equation 21 is different from the coefficient in Light's formula (1941) because of the changes of the units of wind speed U_a and the snow reduction rate and the different location of thermistor and manometer.

The snow depth reduction rate, $\dot{z}_e$ (m day^{-1}), due to the latent heat transport H_e, can be expressed as

$$\dot{z}_e = 1.18 \times 10^{-3}\ U_a\ (e_a - e_s) \qquad \text{for } T_a > 0^{\circ}C \tag{21}$$

where the wind speed U_a is in m sec^{-1}, the vapor pressure e_a of the air is mbars and vapor pressure above the snow surface e_s is in mbars.

Snow melting $\dot{z}_r$ (m day^{-1}), due to the rainfall is developed from the energy balance (Gu and Stefan, 1990), i.e. heat energy released by rain is equal to the heat energy absorbed by the snow

$$\dot{z}_r = \frac{P_r\ \rho_w\ c_p\ T_a}{\lambda_{sw}\ \rho_{sw}} \qquad \text{for } T_a > 0^{\circ}C \tag{22}$$

where P_r is the precipitation (m of water day^{-1}), ρ_w is the water density (kg m^{-3}), and c_p is the specific heat of water (kcal kg^{-1} °C^{-1}), The equation 18,19, 21 and 22 are substituted in equation 17 to determine the overall change in snow thickness.

Prediction of the snow depth is very sensitive to the snow compaction factor C_{sw} and snowfall data. A single compaction factor sometimes is not enough to account the complex snow accumulation which is strongly affected by wind and wind sheltering of a lake. Snowfall data obtained from an off-lake weather station may not representative of the snowfall in the lake.

Appendix B. Ice Thickness Prediction in the Winter Temperature Model

Prediction of the ice thickness is essential to the winter temperature modeling. Ice usually grows up at the ice-water interface, but ice can decay at the snow-ice interface, ice-water interface, and within the ice layer. The change in the ice thickness over one day is given by a mass balance equation

$$\frac{dz_i}{dt} = \dot{z}_{ic} - \dot{z}_{is} - \dot{z}_{ir} \tag{23}$$

where z_i is the ice thickness (m), $\dot{z}_{ic}$ is the ice growth/decay rate (m day^{-1}) due to the conduction/convection, $\dot{z}_{is}$ and $\dot{z}_{ir}$ are the ice thickness reduction rates (m day^{-1}) due to absorbed solar radiation and rainfall, respectively.

The mass balance equation of the ice thickness due to conduction and convection is given by (Ashton, 1986; Gu and Stefan, 1990)

$$\dot{z}_{ic} = \frac{1}{\rho_i \lambda_i}\left[\frac{T_{iw} - T_a}{\frac{z_i}{k_i} + \frac{z_{sw}}{k_{sw}} + \frac{1}{h_{sa}}} - k_w\left(\frac{dT}{dz}\right)_{z=0}\right] \tag{24}$$

where ρ_i is the ice density (kg m^{-3}), λ_i is the latent heat of fusion of ice (kcal kg^{-1}), T_{iw} is the temperature (0°C) at the ice-water interface, k_i is the thermal conductivity of ice (kcal day^{-1} °C^{-1} m^{-1}), k_{sw} is the thermal conductivity of snow (kcal day^{-1} °C^{-1} m^{-1}), k_w is the thermal conductivity of water (kcal day^{-1} °C^{-1} m^{-1}), and h_{sa} is the bulk heat transfer coefficient at the snow/air interface (kcal day^{-1} °C^{-1} m^{-2}) given by (Fertuck et al., 1971)

$$h_{sa} = C_w U_a \tag{25}$$

where U_a is the wind speed in mph, C_w is an empirical coefficient ranging from 0.29 to 0.37 if h_{sa} is in BTU hr^{-1} ft^{-2} $°F^{-1}$, and a value of 0.33 was used in the model (Gu and Stefan, 1990).

In the equation 24, the ice thickness increases (ice growth) if air temperature T_a is less than zero, otherwise the ice thickness decreases (ice decay). Prediction of ice thickness requires to accurately estimate the thermal conduction coefficient of water k_w, water temperature gradient at the ice-water interface, and coefficient C_w for the bulk heat transfer coefficient h_{sa}. Prediction of the ice thickness is sensitive to k_w and temperature gradients at the ice-water interface used in the model. Further investigation is needed in the future.

Internal melting in the ice layer results from internal absorption of solar radiation, can be expressed as

$$\dot{z}_{is} = \frac{H_{is}}{\rho_i \lambda_i} \tag{26}$$

where H_{is} is the absorbed short wave radiation. The shortwave radiation absorbed within the ice is

$$H_{is} = H_{sw} \{\beta_i + (1 - \beta_i)(1 - \alpha_i)[1 - \exp(\mu_i z_i)]\} \tag{27}$$

where H_{sw} is the solar radiation available at the top surface of the ice, β_i is the surface absorption coefficient for ice, α_i is the surface reflectivity for ice, μ_i is the attenuation coefficient in ice, z_i is the ice thickness.

The ice decay rate $\dot{z}_{ir}$ (m day^{-1}), due to the rainfall is developed by the energy balance (similar to equation 22) when snow depth is zero

$$\dot{z}_{ir} = \frac{P_r \rho_w c_p T_a}{\lambda_i \rho_i} \quad \text{for } T_a > 0°C \tag{28}$$

The equation 24, 26, 27 and 28 are substituted in equation 23 to determine the overall change in ice thickness.